Acta of Bioengineering and Biomechanics
Vol. 7, No. 2, 2005

Hip joint lubrication after injury in stochastic description of optimum standard deviations

KRZYSZTOF CH. WIERZCHOLSKI

Base Technique Department, Maritime University of Gdynia, 81-225 Gdynia, ul. Morska 83, Poland

The lubrication parameters of rough and used cartilage surface in human hip joint changes suddenly after its injury. Stochastic changes of the roughness of the surfaces of the head of bone and stochastic changes of the load imply the random changes of gap height. Hence, the pressure distributions and capacity as well as friction forces and friction coefficients radically decrease or increase in several microseconds after trauma. These changes are very difficult to measure, hence an appropriate numerical research in this field is very important. In order to obtain correct numerical results, we have to perform calculations using stochastic description with optimum standard deviations.

Key words: hip joint impulsive lubrication, cartilage roughness, random changes

1. Preliminaries

This paper presents the lubrication of human hip joint under stochastic, unsteady and impulsive conditions. The problem of lubrication of human hip joint after injury under random conditions has not been presented in the papers mentioned in the references: [2], [5]–[9], [13], [16]–[20], [23], [28], [29], [37]. New values of capacities of human hip joint occurring several microseconds after injury very often affect further development of disease or damage to the joint caused by trauma. Therefore the knowledge of lubrication parameters on the grounds of random conditions, for example the changes observed several microseconds after trauma, is necessary for further diagnosis and therapy. The concentrated force P applied onto the external surface of tissue causes an injury to human hip joint.

If the concentrated force P is not great, then the deformations of human body and deformations of rough joint cartilage generate only small changes in gap height of human hip joint (see the head of bone in figure 1a). If the concentrated force is sufficient, e.g. it amounts to 10 P, we can observe a dislocation of the head of bone of human hip joint (figure 1b).

Figure 1c presents early degenerative changes of articular cartilage in human hip joint, while in figure 1c the narrowing of hip gap height is indicated.

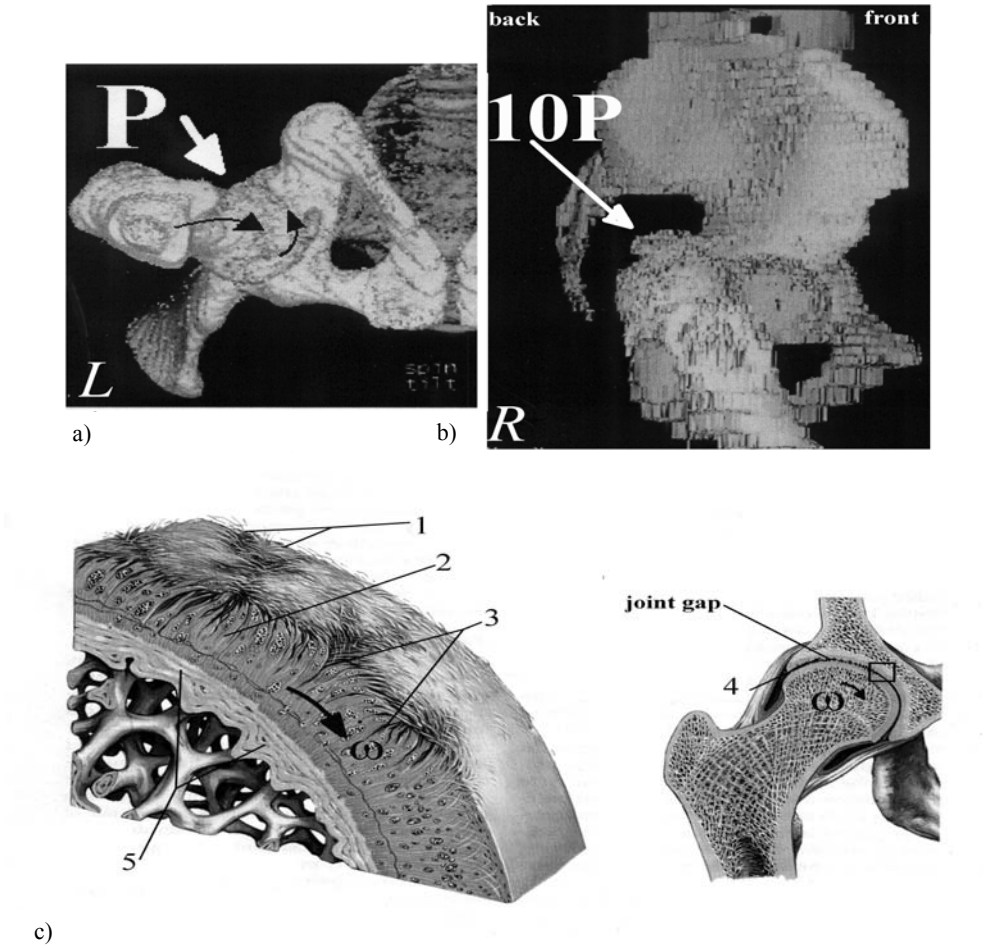

Fig. 1. Negligibly small gap-height changes caused by the force P in human hip joint (a), dislocation of bone head of right hip joint caused by the force $10\times P$ (b), gap space of a joint gap with early degenerations of joint surfaces caused by the fibrillations of cartilage, after Buckwalter, Clinical Symposia, 1995, Vol. 47, 2, 1 – surface fibrillations of cartilage, 2 – early disruptions of matrix molecular framework, 3 – superficial fissures, 4 – roughened articular surfaces and minimal narrowing of joint gap, 5 – sclerosis of subchondral bone (c)

We assume that the semi-infinite region of the sclerosis of subchondral bone (see figure 1c) is occupied by a deformable tissue medium.

2. Governing equations and deformations of gap height

Synovial fluid flow in the gap of a human hip joint is described by the equation of conservation of momentum and the equations of continuity. These equations and the second-order approximation of the general constitutive equation given by Rivlin and Ericksen can be written in the following form:

$$\mathrm{Div}\mathbf{S} = \rho d\mathbf{v}/dt, \quad \mathrm{div}\mathbf{v} = 0, \quad \mathbf{S} = -p\mathbf{I} + \eta_0 \mathbf{A}_1 + \alpha(\mathbf{A}_1)^2 + \beta\mathbf{A}_2, \tag{1}$$

where: $\mathbf{S}$ is the stress tensor, p is the pressure, $\mathbf{I}$ stands for the unit tensor, $\mathbf{A}_1$ and $\mathbf{A}_2$ are the first two Rivlin–Ericksen tensors, η, α, β are three material constants of synovial fluid, and η denotes the viscosity. The tensors $\mathbf{A}_1$ and $\mathbf{A}_2$ are given by symmetric matrices defined by [21], [27]:

$$\mathbf{A}_1 \equiv \mathbf{L} + \mathbf{L}^T, \quad \mathbf{A}_2 \equiv \mathrm{grad}\,\mathbf{a} + (\mathrm{grad}\,\mathbf{a})^T + 2\mathbf{L}^T\mathbf{L}, \quad \mathbf{a} \equiv \mathbf{L}\,\mathbf{v} + \frac{\partial \mathbf{v}}{\partial t}, \tag{2}$$

where: $\mathbf{L}$ is the tensor of gradient fluid velocity vector (s^{-1}), $\mathbf{L}^T$ is the tensor for the transpose of a matrix of gradient vector of an oil (s^{-1}), $\mathbf{v}$ stands for the velocity (m/s), t is the time (s), and $\mathbf{a}$ is the acceleration vector (m/s^2).

It is assumed that the product of the Deborah and Strouhal numbers, i.e. *DeStr*, and the product of the Reynolds number, dimensionless clearance, and the Strouhal number, i.e. $Re\psi Str$, are of the same order. Moreover, $DeStr >> A_\alpha \equiv \alpha\omega/\eta_0$, where ω is the angular velocity of the head of bone. We assume additionally rotational motion of a human head of bone at the peripheral velocity $U = \omega R$, unsymmetrical, unsteady synovial flow in the gap, viscoelastic and unsteady properties of synovial fluid, constant density ρ of the synovial fluid, characteristic value of the gap height ε_0 of hip joint, no slip on the bone surfaces, and R – the radius of the head of bone [30]–[36]. We also assume the relations between dimensional and dimensionless quantities to be in the following form:

$$\begin{gathered} r = \varepsilon_0 r_1, \quad \vartheta = R\vartheta_1, \quad t = t_0 t_1, \quad \varepsilon_T = \varepsilon_0 \varepsilon_{T1}, \quad v_\varphi = U v_{\varphi 1}, \\ v_r \equiv U\psi v_{r1}, \quad v_\vartheta \equiv U v_{\vartheta 1}, \quad p = p_0 p_1, \quad p_0 \equiv U\eta_0 R/(\varepsilon_0)^2 \end{gathered} \tag{3}$$

and the Reynolds number, the modified Reynolds number, the Strouhal and Deborah numbers are as follows:

$$Re \equiv \rho U\varepsilon_0/\eta, \quad Re\psi \equiv \rho\omega(\varepsilon_0)^2/\eta_0, \quad Str \equiv R/Ut_0, \quad De \equiv \beta U/\eta_0 R, \tag{4}$$

$$DeStr = \beta/\eta_0 t_0, \quad Re\psi Str = \rho(\varepsilon_0)^2/\eta_0 t_0. \tag{5}$$

In the case of synovial fluid, the inequality $0 < \beta/t_0 < \eta_0$ is valid and the values of pseudo-viscosity β range mostly from 0.0001 to 0.1000 Pas^2.The dimensionless symbols are marked with the subscript 1. Neglecting the terms representing a radial clearance $\psi \equiv \varepsilon_0/R \approx 10^{-3}$ in the governing equations expressed in the spherical

coordinates r, φ, ϑ and taking into account the above-mentioned assumptions, we have [25]:

$$Re\psi\, Str\frac{\partial v_{\varphi 1}}{\partial t_1} = -\frac{1}{\sin\vartheta_1}\frac{\partial p_1}{\partial\varphi} + \frac{\partial}{\partial r_1}\left(\frac{\partial v_{\varphi 1}}{\partial r_1}\right) + DeStr\frac{\partial^3 v_{\varphi 1}}{\partial t_1 \partial r_1^2}, \tag{6}$$

$$0 = \frac{\partial p_1}{\partial r_1}, \tag{7}$$

$$Re\psi\, Str\frac{\partial v_{\vartheta 1}}{\partial t_1} = -\frac{\partial p_1}{\partial\vartheta_1} + \frac{\partial}{\partial r_1}\left(\frac{\partial v_{\vartheta 1}}{\partial r_1}\right) + DeStr\frac{\partial^3 v_{\vartheta 1}}{\partial t_1 \partial r_1^2}, \tag{8}$$

$$\frac{\partial v_{\varphi 1}}{\partial\varphi} + \sin(\vartheta_1)\frac{\partial v_{r1}}{\partial r_1} + \frac{\partial}{\partial\vartheta_1}\left[v_{\vartheta 1}\sin(\vartheta_1)\right] = 0, \tag{9}$$

where: $0 \le \varphi \le 2\pi\theta_1$, $0 \le \theta_1 \le 1$, $\pi/8 \le \vartheta_1 \le \pi/2$, $0 \le r_1 \le \varepsilon_{T1}$, ε_{T1} is the dimensionless total gap height. The symbols $v_{\varphi 1}$, v_{r1}, $v_{\vartheta 1}$ denote the components of dimensionless synovial fluid velocity in circumferential, gap-height and meridional directions of bone head, respectively.

Figure 2a shows the changes in the space of joint gap height caused by vibrations in unsteady impulsive motion [1], [3], [10]–[12], [21], [26], [27], [38]. The unsteady impulse, which is generated at the very beginning, vanishes after infinite time and the head of bone assumes a stationary position (see figure 2b). The diagrams of the distribution of time-dependent velocity and pressure are presented in figure 2c. Figure 2d shows the random effects of roughness and undulation caused by the random fibrillation of cartilage surfaces and by sclerosis of subchondral bone. The dimensionless gap height ε_{T1} depends on the variables φ and ϑ and the time t and consists of two parts [24], [36]:

$$\varepsilon_{T1} = \varepsilon_{T1s}(\varphi, \vartheta, t) + \delta_1(\varphi, \vartheta, \xi), \tag{10}$$

where ε_{T1s} denotes a total dimensionless nominally smooth part of the area of thin fluid layer. This part of the gap height contains dimensionless corrections of gap height caused by the hyperelastic cartilage deformations. The symbol δ_1 denotes the dimensionless random part of the changes of gap height resulting from the vibrations, unsteady loading and surface roughness asperities of cartilage measured from a nominal mean level (see figure 2d). The symbol ξ describes the random variable, which characterizes the roughness arrangement. Expectancy operator is defined by:

$$\mathrm{E}(*) = \int_{-\infty}^{+\infty} (*) \times f_k(\delta_1) d\delta_1, \tag{11}$$

where f_k describes a dimensionless function of the probability density.

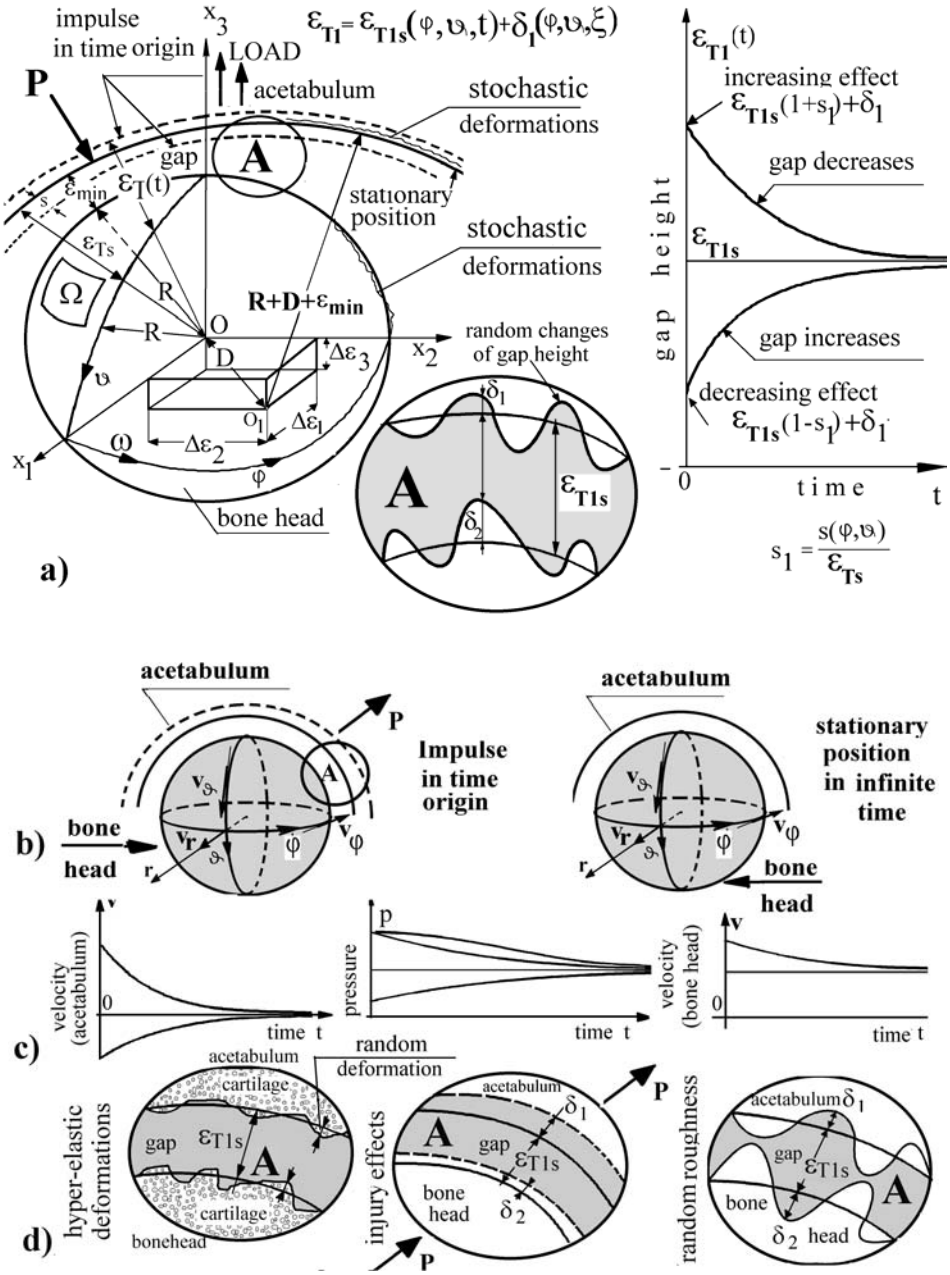

Fig. 2. Lubrication region, eccentricities, gap height variations with the time after injury (a), position of bone head in stationary and impulsive motion (b), diagrams of pressure and velocity of synovial fluid distributions versus time (c), stochastic deformations of cartilage, results of impact and random roughness (d)

3. Optimization of standard deviation of gap height

A real description of the gap height changes depends on the variations of cartilage surface. Random changes of cartilage surface are described by the probability density functions on the basis of comparison between the results of the experiments of this author and these reported by DOWSON and MOW [2], [17], [23] (see figures 3a, b, 4a, b). The measurements of the changes on the sample surface (10 mm × 10 mm) of a pathological cartilage resting on the sphere (see figure 3a, b) of the head of bone in human hip joint have been performed with microsensor laser installed in Rank-Taylor-Hobson-Talyscan-150 Apparatus and processed by means of the Talymap Expert and Microsoft Exel Computer Program. The measurements of the values of asperities on the sample surface (2 mm × 2 mm) of normal cartilage of the head of bone in human hip joint have been carried out with a mechanical sensor (figure 4a, b). A proper description of the random changes in a gap height depends on an appropriate selection of probability density function. As a criterion of estimation we choose the standard deviation. The probability density functions presented in figures 3c and 4c refer to the changes of cartilage surface caused by vibrations and roughness, respectively. We assume that the dimensionless distribution of probability density function for random changes of joint gap has the following sequential form [4], [24]:

$$f_k(\delta_1) \equiv \begin{cases} \dfrac{m_{k1}}{c_{k1}^{2k+1}}(c_{k1}^2 - \delta_1^2)^k & \text{for } -c_{k1} \le \delta_1 \le +c_{k1}, \\ 0 & \text{for } \quad |\delta_1| > c_{k1}, \end{cases} \tag{12}$$

where $k = 1, 3, 5, 7, \ldots$ Because the probability cannot be greater than unity, we have:

$$f_k(\delta_1) \le 1 \Rightarrow m_{k1} \le c_{k1}. \tag{13}$$

The symbol m_{k1} denotes the unknown constant values. The dimensionless coefficient c_{k1} indicates the limits of the random changes of the joint gap within the interval $-c_{k1} \le \delta_1 \le c_{k1}$. The dimensional values are as follows: $c_k = \varepsilon_0 c_{k1}$, $\delta = \varepsilon_0 \delta_1$. To determine the unknown dimensionless value m_{k1} we make use of the known property of the probability function [4], [24]:

$$\int_{-\infty}^{+\infty} f_k(\delta_1) d\delta_1 = 1 \Leftrightarrow \int_{-c_{k1}}^{c_{k1}} f_k(\delta_1)\, d\delta_1 = 1. \tag{14}$$

We insert function (12) into formula (14) and assume a new dimensionless variable y_1:

$$\delta_1 = y_1 c_{k1} \Rightarrow d\delta_1 = c_{k1}\, dy_1. \tag{15}$$

Hence from equation (14) after simple calculations we obtain:

$$m_{k1} = \left(\int_{-1}^{+1} (1 - y_1^2)^k \, dy_1 \right)^{-1}. \tag{16}$$

After integration from equations (14), (16) it follows:

$$m_{k1} = \frac{1}{2} \left[\sum_{s=0}^{k} \frac{(-1)^s}{2s+1} \left(\frac{k!}{s!(k-s)!} \right) \right]^{-1} \le c_{k1}, \quad k = 1, 3, 5, 7, ... \tag{17}$$

From (17) we obtain:

$$\begin{gathered} m_{11} = \frac{3}{4}, \quad m_{31} = \frac{35}{32}, \quad m_{51} = \frac{693}{512}, \quad m_{71} = \frac{6435}{4096}, ..., \\ c_{11} \ge 0.7500, \quad c_{31} \ge 1.09375, \quad c_{51} \ge 1.35315, \quad c_{71} \ge 1.571044, ... \end{gathered} \tag{18}$$

The sequence of probability density functions and its limits are presented in Appendix 1.

The standard deviation has the following form [24]:

$$\sigma_{k1} = \sqrt{E(X^2) - E^2(X)}. \tag{19}$$

The expectancy operators are defined as follows[4], [24]:

$$\mathrm{E}(X) \equiv \int_{-\infty}^{+\infty} \delta_1 \frac{m_{k1}}{c_{k1}} \left(1 - \frac{\delta_1^2}{c_{k1}^2} \right)^k d\delta_1 = 0, \tag{20}$$

$$\mathrm{E}(X^2) \equiv \int_{-\infty}^{+\infty} \delta_1^2 \frac{m_{k1}}{c_{k1}} \left(1 - \frac{\delta_1^2}{c_{k1}^2} \right)^k d\delta_1. \tag{21}$$

Taking into account a new variable (15) we obtain:

$$\mathrm{E}(X^2) = 2 m_{k1} c_{k1}^2 \int_0^1 y_1^2 (1 - y_1^2)^k \, dy_1 = 2 m_{k1} c_{k1}^2 \sum_{s=0}^{k} \frac{(-1)^s}{2s+3} \frac{k!}{s!(k-s)!}. \tag{22}$$

We insert the result (17) into (22), and (22) into (19). Thus we obtain the sequence of standard deviations in the form:

$$\sigma_{k1} = c_{k1} \sqrt{\frac{\displaystyle\sum_{s=0}^{k} \frac{(-1)^s}{2s+3} \frac{k!}{s!(k-s)!}}{\displaystyle\sum_{s=0}^{k} \frac{(-1)^s}{2s+1} \frac{k!}{s!(k-s)!}}} \quad \text{for} \quad k = 1, 3, 5, 7, ... \tag{23}$$

By virtue of (23) and (18) we have:

$$\sigma_{11}=\frac{c_{11}}{\sqrt{5}}\geq\frac{3}{4\sqrt{5}}=0.335,\quad \sigma_{31}=\frac{c_{31}}{\sqrt{9}}\geq\frac{35}{96}=0.364,$$
$$\sigma_{51}=\frac{c_{51}}{\sqrt{13}}\geq\frac{693}{512\sqrt{13}}=0.3754,\quad \sigma_{71}=\frac{c_{71}}{\sqrt{17}}\geq\frac{6435}{4096\sqrt{17}}=0.3810. \tag{24}$$

The limits of standard deviations have the form (Appendix 2):

$$\lim_{k\to\infty}\sigma_{k1}=\frac{1}{\sqrt{2\pi}}. \tag{25}$$

• If the vibrations and unsteady load cause random changes in the height of the joint gap, then the range of each probability density function of changes has a different value. Each probability density function assumes the value of unity in one point of its domain (figure 3c). In this case, we insert equation (18) into equation (12) or (A1.1) and obtain the following probability density functions and their standard deviations [22]:

$$f_1(\delta_1)\equiv\begin{cases}\left[1-\left(\dfrac{4\delta_1}{3}\right)^2\right] & \text{for } |\delta_1|\leq+3/4,\\ 0 & \text{for } |\delta_1|>3/4,\end{cases}\quad \sigma_{11}=\frac{3/4}{\sqrt{5}}=0.336;$$

$$f_3(\delta_1)\equiv\begin{cases}\left[1-\left(\dfrac{32\delta_1}{35}\right)^2\right]^3 & \text{for } |\delta_1|\leq+35/32=1.09375,\\ 0 & \text{for } |\delta_1|>1.09375,\end{cases}\quad \sigma_{31}=\frac{35}{32\sqrt{9}}=0.364583;$$

$$f_5(\delta_1)\equiv\begin{cases}\left[1-\left(\dfrac{512\delta_1}{693}\right)^2\right]^5 & \text{for } |\delta_1|\leq+\dfrac{693}{512}=1.353515,\\ 0 & \text{for } |\delta_1|>1.353515,\end{cases}\quad \sigma_{51}=\frac{693}{512\sqrt{13}}=0.375397;$$

$$f_7(\delta_1)\equiv\begin{cases}\left[1-\left(\dfrac{4096\delta_1}{6435}\right)^2\right]^7 & \text{for } |\delta_1|\leq+\dfrac{6435}{4096}=1.571044,\\ 0 & \text{for } |\delta_1|>1.57,\end{cases}\quad \sigma_{71}=\frac{6435}{4096\sqrt{17}}=0.381034;$$

$$f_{\infty1}=e^{-\pi\delta_1^2}\quad \text{for } -\infty<\delta_1<\infty,\quad \sigma_{\infty1}=\frac{1}{\sqrt{2\pi}}=0.4418. \tag{26}$$

The distributions of probability density functions and their standard deviations are presented in figure 3c. We can choose the function with the least standard deviation.

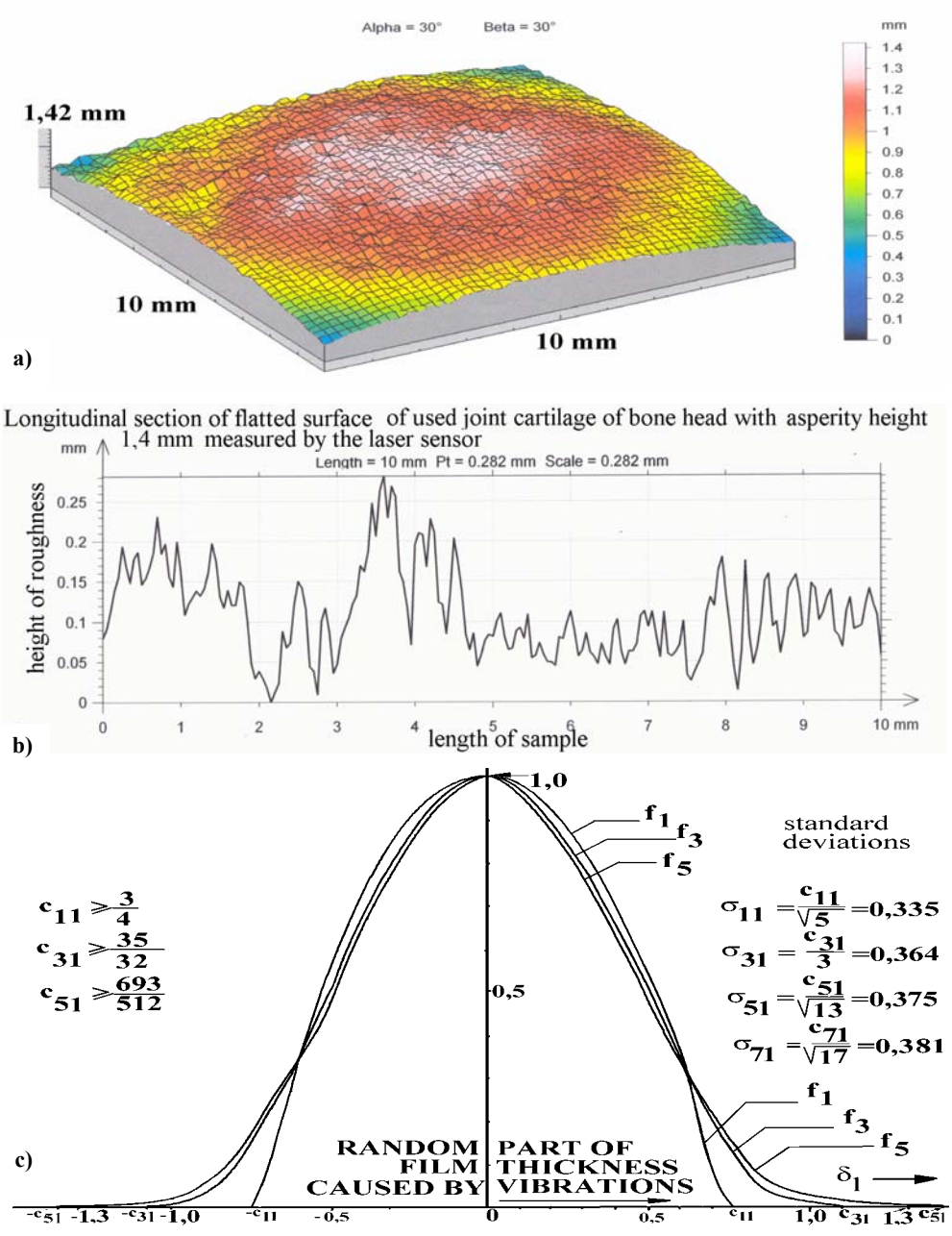

Fig. 3. Measurement of roughness on the sample surface (10 mm × 10 mm) of used and pathological cartilage taken from bone head of human hip joint (a). Longitudinal section of flattened surface of used joint cartilage of bone head with the asperity height of 1.4 mm measured by the laser sensor (b). Distributions of probability density functions of random changes of gap height of human hip joint caused by vibration and unsteady load on the cartilage surface (c)

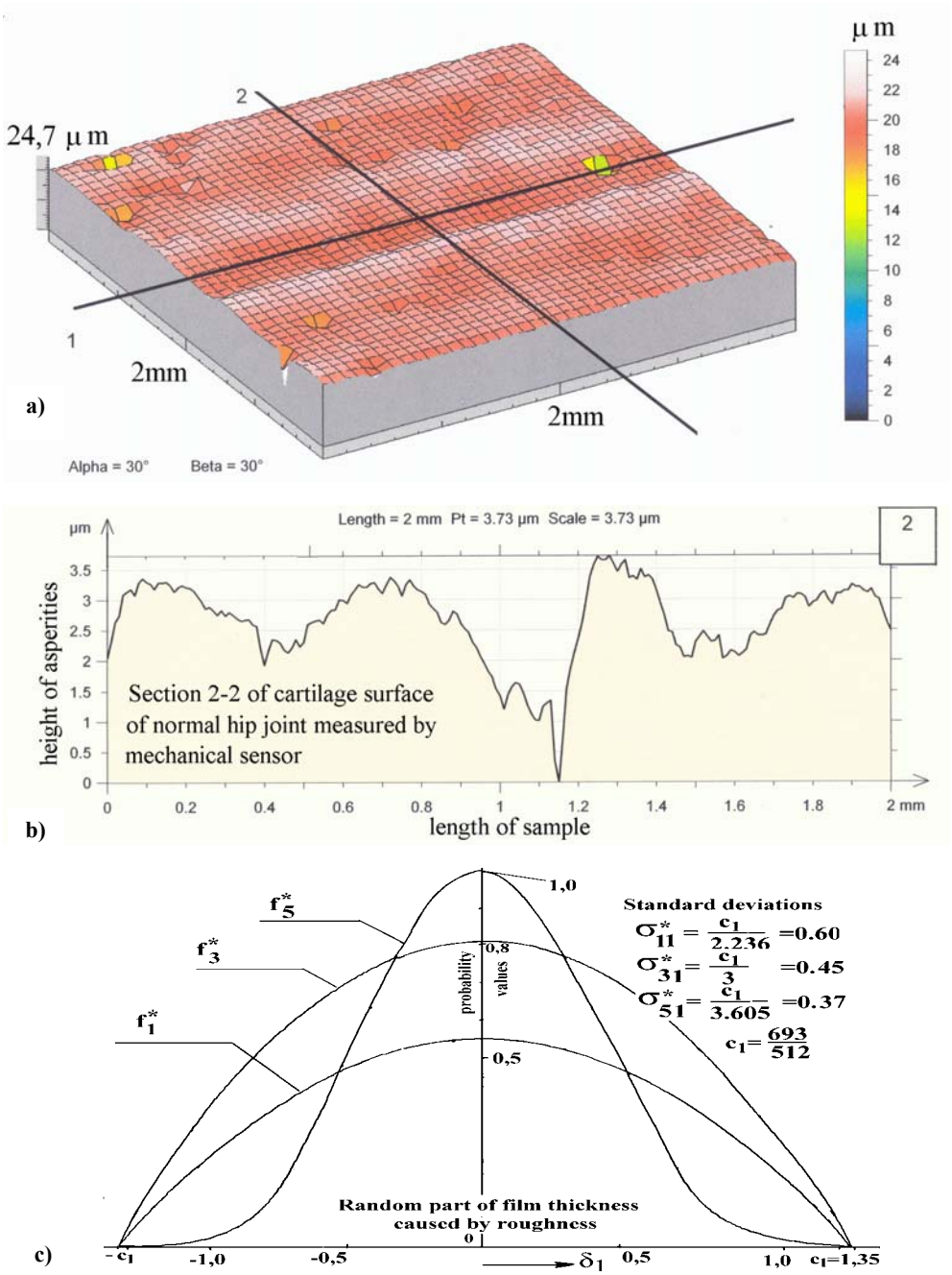

Fig. 4. Measurement of roughness of a normal cartilage sample (2 mm × 2 mm) taken from bone head of human hip joint (a). Asperities of normal cartilage surface along the cross section 2-2 of a normal cartilage sample (b). Distributions of probability density functions of random changes of gap height of hip joint caused by asperities of roughness on the cartilage surfaces (c)

• If the random changes in the height of the joint gap are caused by the asperities of cartilage surface roughness, then the range of each of the probability density functions has the same value (see figure 4c). If we insert the dimensionless constant value $c_{k1} = c_1 = 693/512 = 1.353515$ into the probability density functions (12) or (A1.1), then the probability density functions and standard deviations in the dimensionless form are as follows:

$$f_1^*(\delta_1) \equiv \begin{cases} \dfrac{3}{4c_1}\left(1-\dfrac{\delta_1^2}{c_1^2}\right) & \text{for } -c_1 \le \delta_1 \le +c_1, \\ 0 & \text{for } |\delta_1| > c_1, \end{cases} \quad \sigma_{11}^* = \frac{c_1}{\sqrt{5}} = 0.605310;$$

$$f_3^*(\delta_1) \equiv \begin{cases} \dfrac{35}{32\,c_1}\left(1-\dfrac{\delta_1^2}{c_1^2}\right)^3 & \text{for } -c_1 \le \delta_1 \le +c_1, \\ 0 & \text{for } |\delta_1| > c_1, \end{cases} \quad \sigma_{31}^* = \frac{c_1}{\sqrt{9}} = 0.451171 \ ; \quad (27)$$

$$f_5^*(\delta_1) \equiv \begin{cases} \dfrac{693}{512c_1}\left(1-\dfrac{\delta_1^2}{c_1^2}\right)^5 & \text{for } -c_1 \le \delta_1 \le +c_1, \\ 0 & \text{for } |\delta_1| > c_1, \end{cases} \quad \sigma_{51}^* = \frac{c_1}{\sqrt{13}} = 0.375397.$$

All the functions have positive values for $|\delta_1| < c_1$ and zero values for $|\delta_1| > c_1$. In this case, the distributions of probability density functions of gap-height changes are presented in figure 4c. The sequence of probability density functions tends to an optimal boundary function which takes the value of unity in the middle point of its domain. This function attains the least standard deviation.

4. The method of integration applied to hydrodynamic problem

We introduce a new dimensionless variable [14], [15], [25]:

$$\chi \equiv r_1 N, \quad N \equiv \frac{1}{2}\sqrt{\frac{Re\psi\, Str}{t_1}}, \quad t_1 > 0, \quad 0 < \frac{DeStr}{t_1} < 1 \qquad (28)$$

and we assume solutions of the system (6)–(9) to be in the form of the following convergent series[3], [17]:

$$v_{\varphi 1} = v_{\varphi 0\Sigma}(\chi, \varphi, \vartheta_1) + \frac{DeStr}{t_1} v_{\varphi 1\Sigma}(\chi, \varphi, \vartheta_1) + \left(\frac{DeStr}{t_1}\right)^2 v_{\varphi 2\Sigma}(\chi, \varphi, \vartheta_1) + \ldots, \qquad (29)$$

$$v_{\vartheta 1} = v_{\vartheta 0\Sigma}(\chi,\varphi,\vartheta_1) + \frac{DeStr}{t_1} v_{\vartheta 1\Sigma}(\chi,\varphi,\vartheta_1) + \left(\frac{DeStr}{t_1}\right)^2 v_{\vartheta 2\Sigma}(\chi,\varphi,\vartheta_1) + \ldots, \tag{30}$$

$$v_{r1} = v_{r0\Sigma}(\chi,\varphi,\vartheta_1) + \frac{DeStr}{t_1} v_{r1\Sigma}(\chi,\varphi,\vartheta_1) + \left(\frac{DeStr}{t_1}\right)^2 v_{r2\Sigma}(\chi,\varphi,\vartheta_1) + \ldots, \tag{31}$$

$$p_1 = p_{10}(\varphi,\vartheta_1,t_1) + \frac{DeStr}{t_1} p_{11}(\varphi,\vartheta_1,t_1) + \left(\frac{DeStr}{t_1}\right)^2 p_{12}(\varphi,\vartheta_1,t_1) + \ldots, \tag{32}$$

where $t_1 > 0$, $0 < DeStr << 1$, $(DeStr/t_1) < 1$. In equations (6)–(8), we replace the derivatives with respect to the variables t_1, r_1 by the derivatives with respect to the one variable χ only, using the following relations:

$$\frac{\partial}{\partial t_1} = \frac{\partial}{\partial \chi}\frac{\partial \chi}{\partial t_1} = -\frac{1}{4}\sqrt{Re\psi\, Str}\,\frac{r_1}{t_1\sqrt{t_1}}\frac{\partial}{\partial \chi} = -\frac{\chi}{2t_1}\frac{\partial}{\partial \chi}, \tag{33}$$

$$\frac{\partial^2}{\partial r_1^2} = \frac{\partial}{\partial r_1}\left(\frac{\partial}{\partial r_1}\right) = \frac{\partial}{\partial \chi}\left(\frac{\partial}{\partial \chi}\frac{\partial \chi}{\partial r_1}\right)\frac{\partial \chi}{\partial r_1} = \frac{Re\psi\, Str}{4t_1}\frac{\partial^2}{\partial \chi^2}, \tag{34}$$

$$\frac{\partial^3}{\partial t_1 \partial r_1^2} = \frac{\partial}{\partial t_1}\left(\frac{Re\psi\, Str}{4t_1}\frac{\partial^2}{\partial \chi^2}\right) = -\frac{Re\psi\, Str}{4t_1^2}\frac{\partial^2}{\partial \chi^2} + \frac{Re\psi\, Str}{4t_1}\frac{\partial}{\partial \chi}\left(\frac{\partial^2}{\partial \chi^2}\right)\frac{\partial \chi}{\partial t_1}$$
$$= -\frac{Re\psi\, Str}{4t_1^2}\left(\frac{\partial^2}{\partial \chi^2} + \frac{\chi}{2}\frac{\partial^3}{\partial \chi^3}\right). \tag{35}$$

Afterwards we insert the series (29)–(32) into the changed system (6)–(9), where the variables t_1, r_1 are replaced by the variable χ. Moreover, we equate the terms multiplied by the same powers of the parameter $(DeStr/t_1)^k$ for $k = 0, 1, 2, \ldots$ Thus we obtain the following sequence of systems of ordinary differential equations:

$$\frac{d^2 v_{i0\Sigma}}{d\chi^2} + 2\chi\frac{dv_{i0\Sigma}}{d\chi} = \frac{1}{N_i^2}\frac{\partial p_{10}}{\partial \alpha_i}, \tag{36}$$

$$\frac{d^2 v_{i1\Sigma}}{d\chi^2} + 2\chi\frac{dv_{i1\Sigma}}{d\chi} + 4(v_{i1\Sigma}) = \frac{1}{N_i^2}\frac{\partial p_{11}}{\partial \alpha_i} + \frac{d^2 v_{i0\Sigma}}{d\chi^2} + \frac{\chi}{2}\frac{d^3 v_{i0\Sigma}}{d\chi^3}, \tag{37}$$

$$\frac{d^2 v_{i2\Sigma}}{d\chi^2} + 2\chi\frac{dv_{i2\Sigma}}{d\chi} + 8(v_{i2\Sigma}) = \frac{1}{N_i^2}\frac{\partial p_{12}}{\partial \alpha_i} + 2\frac{d^2 v_{i1\Sigma}}{d\chi^2} + \frac{1}{2}\chi\frac{d^3 v_{i1\Sigma}}{d\chi^3}, \tag{38}$$

where $i = \varphi, \vartheta$; $\alpha_\varphi \equiv \varphi$, $\alpha_\vartheta \equiv \vartheta_1$ and:

$$(N_\varphi)^2 \equiv N^2 \sin(\vartheta_1), \quad N_\vartheta \equiv N. \tag{39}$$

5. Final solutions for unsteady lubrication

The general and particular solutions for the ordinary differential equations (36) under proper boundary conditions have been derived in Appendix 3. We insert constants (A3.9) into general solution (A3.1) for synovial fluid velocity components. Hence the synovial fluid velocity components (29), (30) in circumference and meridional directions have the following final forms:

$$v_{\varphi 1} = \sin\vartheta_1 - \frac{\sin\vartheta_1 + v_{\varphi 03}\left[\chi = \varepsilon_{T1}N\right]}{v_{01}\left[\chi = \varepsilon_{T1}N\right]} v_{01}(\chi) + v_{\varphi 03}(\chi) + O(DeStr), \tag{40}$$

$$v_{\vartheta 1} = -\frac{v_{\vartheta 03}\left[\chi = \varepsilon_{T1}N\right]}{v_{01}\left[\chi = \varepsilon_{T1}N\right]} v_{01}(\chi) + v_{\vartheta 03}(\chi) + O(DeStr), \tag{41}$$

$$0 \le \chi_1 \le \varepsilon_{T1}N, \quad \chi = Nr_1, \quad N \equiv 0.5(StrRe\psi)^{0.5},$$

$$0 < t_1 < \infty, \quad 0 \le r_1 \le \varepsilon_{T1}, \quad \pi/8 \le \vartheta_1 \le \pi/2, \quad 0 < \varphi < 2\pi\theta_1, \quad 0 \le \theta_1 < \infty.$$

By virtue of solutions (40), (41), the particular velocity components of synovial fluid in φ and ϑ directions for unsteady flow have the following dimensionless forms:

$$v_{\varphi 0\Sigma}(\varphi, r_1, \vartheta_1, t_1) = +\sin\vartheta_1 - \left\{\sin\vartheta_1 - \frac{\sqrt{\pi}}{2N^2\sin\vartheta_1}\frac{\partial p_{10}}{\partial\varphi} Y(\chi = N\varepsilon_{T1})\right\}$$
$$\times \frac{\operatorname{erf}(r_1 N)}{\operatorname{erf}(\varepsilon_1 N)} - \frac{\sqrt{\pi}}{2N^2\sin\vartheta_1}\frac{\partial p_{10}}{\partial\varphi} Y(\chi = Nr_1), \tag{42}$$

$$v_{\vartheta 0\Sigma}(\varphi, r_1, \vartheta_1, t_1) = \frac{\sqrt{\pi}}{2N^2}\frac{\partial p_{10}}{\partial\vartheta_1} Y(\chi = N\varepsilon_{T1})$$
$$\times \frac{\operatorname{erf}(r_1 N)}{\operatorname{erf}\left(N\varepsilon_{T1}\right)} - \frac{\sqrt{\pi}}{2N^2}\frac{\partial p_{10}}{\partial\vartheta_1} Y(\chi = Nr_1), \tag{43}$$

$$Y(\chi) \equiv \int_0^{\chi} e^{\chi_1^2}\operatorname{erf}\chi_1 d\chi_1 - \operatorname{erf}\chi\int_0^{\chi} e^{\chi_1^2} d\chi_1, \tag{44}$$

$$N \equiv \frac{1}{2}\sqrt{\frac{Re\psi\, Str}{t_1}}, \quad \operatorname{erf}(\chi_1) = \frac{2}{\sqrt{\pi}}\int_0^{\chi_1} e^{-\chi_2^2} d\chi_2, \tag{45}$$

and $0 \le t_1 < \infty$, $0 \le r_1 \le \varepsilon_{T1}$, $\pi/8 \le \vartheta_1 \le \pi/2$, $0 < \varphi < 2\pi\theta_1$, $0 \le \theta_1 < \infty$, $0 \le \chi_2 \le \chi_1 \le \chi \equiv r_1 N \le \varepsilon_{T1}N \equiv M$, $\varepsilon_{T1} = \varepsilon_{T1}(\varphi, \vartheta_1, t_1)$. We insert the velocity components (42), (43) into the continuity equation (9) and integrate both sides of this equation with respect to the variable r_1. The component of the synovial fluid velocity $v_{r0\Sigma}$ in the gap-height direction equals zero on the surface of the head of bone. Therefore after imposing the

boundary condition $v_{r0\Sigma} = 0$ for $r_1 = 0$, the synovial fluid velocity component in the gap-height direction has the following form:

$$v_{r0\Sigma}(\varphi, r_1, \vartheta_1, t_1)$$

$$= -\frac{Ne^{-\varepsilon_{T1}^2 N^2}}{\operatorname{erf}(h_1 N)}\left[\frac{\partial \varepsilon_{T1}}{\partial \varphi} - \frac{\sqrt{\pi}}{2}\left(\frac{1}{\sin^2 \vartheta_1}\frac{\partial \varepsilon_{T1}}{\partial \varphi}\frac{\partial p_{10}}{\partial \varphi} + \frac{\partial \varepsilon_{T1}}{\partial \vartheta_1}\frac{\partial p_{10}}{\partial \vartheta_1}\right)\frac{1}{N}\int_0^{\varepsilon_{T1}N} e^{\chi_1^2}\operatorname{erf}\chi_1 d\chi_1\right]^r$$

$$\cdot \int_0^{r_1} \frac{\operatorname{erf}(r_2 N)}{\operatorname{erf}(\varepsilon_{T1} N)} dr_2 - \frac{\sqrt{\pi}}{2}\left(\frac{1}{\sin^2 \vartheta_1}\frac{\partial^2 p_{10}}{\partial \varphi^2} + \frac{\partial^2 p_{10}}{\partial \vartheta_1^2} + \frac{\partial p_{10}}{\partial \vartheta_1}\cot \vartheta_1\right)$$

$$\cdot \left\{\frac{1}{N^2} Y(\chi = h_1 N)\int_0^{r_1} \frac{\operatorname{erf}(r_1 N)}{\operatorname{erf}(h_1 N)} dr_1 - \int_0^{r_1} Y(\chi_1 = r_2 N)\, dr_2\right\}, \tag{46}$$

where: $0 \le t_1 < \infty$, $0 \le r_2 \le r_1 \le \varepsilon_{T1}$, $\pi/8 \le \vartheta_1 \le \pi/2$, $0 < \varphi < 2\pi\theta_1$, $0 \le \theta_1 < 1$, $0 \le \chi_2 \le \chi_1 \le \chi \equiv r_1 N \le \varepsilon_{T1} N \equiv M$.

The component of the synovial fluid velocity $v_{r0\Sigma}$ in the gap-height direction does not equal zero on the acetabulum surface. Therefore integrating the continuity equation (9) with respect to the variable r_1 and imposing the boundary condition (A3.7) for $r_1 = \varepsilon_1$ on the velocity component in gap-height direction and taking into account conditions (A3.6) for $r_1 = 0$, we arrive at the following equation:

$$\frac{1}{\sin \vartheta_1}\frac{\partial}{\partial \varphi}\int_0^{\varepsilon_{T1}} v_{\varphi 0\Sigma} dr_1 + \frac{1}{\sin \vartheta_1}\frac{\partial}{\partial \vartheta_1}\int_0^{\varepsilon_{T1}} \sin \vartheta_1 v_{\vartheta 0\Sigma} dr_1 = -Str\frac{\partial \varepsilon_{T1}}{\partial t_1}. \tag{47}$$

6. Stochastic Reynolds equation

If we insert expressions (42)–(43) into (47) and take the expected values of both sides of equation (47), then we obtain the following modified Reynolds equation:

$$\frac{\sqrt{\pi}}{2N^2}\frac{1}{\sin \vartheta_1}\mathrm{E}\left\{\frac{\partial}{\partial \varphi}\left[J(\varepsilon_{T1}N)\frac{\partial p_{10}}{\partial \varphi}\right]\right\} + \frac{\sqrt{\pi}}{2N^2}\mathrm{E}\left\{\frac{\partial}{\partial \vartheta_1}\left[J(\varepsilon_{T1}N)\frac{\partial p_{10}}{\partial \vartheta_1}\sin \vartheta_1\right]\right\}$$

$$= -(\sin \vartheta_1)\mathrm{E}\left\{\frac{\partial}{\partial \varphi}H(\varepsilon_{T1}N)\right\} - Str\frac{\partial \mathrm{E}(\varepsilon_{T1})}{\partial t_1}\sin \vartheta_1, \tag{48}$$

where:

$$J(\varepsilon_{T1}N) \equiv W(\varepsilon_{T1}N)Y(\varepsilon_{T1}N) - \int_0^{\varepsilon_{T1}} Y(r_1 N) dr_1, \qquad H(\varepsilon_{T1}N) \equiv \varepsilon_{T1} - W(\varepsilon_{T1}N), \tag{49}$$

$$W(\varepsilon_{T1}N) \equiv \frac{\int_0^{\varepsilon_{T1}} \operatorname{erf}(r_1 N)dr_1}{\operatorname{erf}(\varepsilon_{T1}N)}, \tag{50}$$

and $\varepsilon_{T1} = \varepsilon_{T1s}(\varphi, \vartheta_1, t_1) + \delta_1$, $0 \le r_2 \le r_1 \le \varepsilon_{T1}$, $0 \le \varphi < 2\pi\theta_1$, $0 \le \theta_1 < 1$, $\pi/8 \le \vartheta_1 \le \pi/2$, $0 \le t_1 < \infty$, $0 \le \chi_2 \le \chi_1 \le \varepsilon_{T1}N$, $0 \le N(t_1) = 0.5(Res/t_1)^{0.5} < \infty$.The modified Reynolds equation (48) determines an unknown time-dependent pressure function $p_{10}(\varphi, \vartheta_1, t_1)$ with stochastic changes.

By using the optimal function of probability density distribution $f_5^* \equiv f_1$ for the stochastic gap-height changes caused by the roughness (see equation (27)), a mean value of total film thickness $\mathrm{E}(\varepsilon_{T1})$ and a mean value of pressure function $\mathrm{E}(p_{10})$ can be presented based on the expectancy operator in the following form [24]:

$$\mathrm{E}(*) = \int_{-\infty}^{+\infty} (*) \times f(\delta_1)d\delta_1, \quad f(\delta_1) \equiv \begin{cases} \left(1 - \dfrac{\delta_1^2}{c_1^2}\right)^5 & \text{for } -c_1 \le \delta_1 \le +c_1, \\ 0 & \text{for } |\delta_1| > c_1, \end{cases} \quad \sigma_1 = \frac{c_1}{\sqrt{13}} = 0.375, \tag{51}$$

where the symbol $c_1 = 1.353515$ denotes the half total range of random variable of the thin layer thickness for normal hip joint (figure 4c). The symbol $\sigma_1 = 0.37539$ is the dimensionless standard deviation. To obtain a dimensional value of the standard deviation σ we must multiply σ_1 by the characteristic value of gap height $\varepsilon_0 = 10 \cdot 10^{-6}$ m. In this case, the dimensional standard deviation equals 3.7 μ. Based on the measurements we found that the value of standard deviation for normal cartilage approached 3.5 μ.

Taking into account equation (51) we can write equation (48) in the form:

$$\begin{aligned} &\frac{\sqrt{\pi}}{2N^2}\frac{1}{\sin\vartheta_1}\frac{\partial}{\partial\varphi}\left\{\int_{-c_1}^{+c_1}\left[\left(1-\frac{\delta_1^2}{c_1^2}\right)^5 J(\varepsilon_{T1}N)\right]d\delta_1\frac{\partial p_{10}}{\partial\varphi}\right\} + \frac{\sqrt{\pi}}{2N^2}\frac{\partial}{\partial\vartheta_1} \\ &\quad \cdot\left\{\int_{-c_1}^{+c_1}\left[\left(1-\frac{\delta_1^2}{c_1^2}\right)^5 J(\varepsilon_{T1}N)\right]d\delta_1\frac{\partial p_{10}}{\partial\vartheta_1}\sin\vartheta_1\right\} \\ &= -(\sin\vartheta_1)\frac{\partial}{\partial\varphi}\left\{\int_{-c_1}^{+c_1}\left(1-\frac{\delta_1^2}{c_1^2}\right)^5 H(\varepsilon_{T1}N)d\delta_1\right\} \\ &\quad - Str\frac{\partial}{\partial t_1}\left[\int_{-c_1}^{+c_1}\left(1-\frac{\delta_1^2}{c_1^2}\right)^5(\varepsilon_{T1s}+\delta_1)d\delta_1\right]\sin\vartheta_1, \end{aligned} \tag{52}$$

where $-c_1 \le \delta_1 \le c_1$, $0 \le \varphi \le 2\pi$, $\pi/8 \le \vartheta_1 \le \pi/2$. We expand the function J into the Taylor series in the neighbourhood of the point $\delta_1 = 0$ in the following form:

$$J(\varepsilon_{T1}N) = J(\varepsilon_{T1s}N) + \frac{\delta_1}{1!}\left(\frac{\partial J(\varepsilon_{T1}N)}{\partial \delta_1}\right)_{\delta_1=0} + \frac{\delta_1^2}{2!}\left(\frac{\partial^2 J(\varepsilon_{T1}N)}{\partial \delta_1^2}\right)_{(\delta_1=0)} + \ldots, \quad (53)$$

$$H(\varepsilon_{T1}N) = \varepsilon_{T1s} - W(\varepsilon_{T1s}N) + \frac{\delta_1}{1!}\left(\frac{\partial H(\varepsilon_{T1}N)}{\partial \delta_1}\right)_{\delta_1=0} - \frac{\delta_1^2}{2!}\left(\frac{\partial^2 W(\varepsilon_{T1}N)}{\partial \delta_1^2}\right)_{\delta_1=0} + \ldots \quad (54)$$

Integrating the functions with respect to the variable δ_1 in equation (52) we obtain:

$$\frac{\sqrt{\pi}}{2N^2}\frac{1}{\sin\vartheta_1}\frac{\partial}{\partial\varphi}\left[I(\varepsilon_{T1}N)\frac{\partial p_{10}}{\partial\varphi}\right] + \frac{\sqrt{\pi}}{2N^2}\frac{\partial}{\partial\vartheta_1}\left[I(\varepsilon_{T1}N)\frac{\partial p_{10}}{\partial\vartheta_1}\sin\vartheta_1\right]$$

$$= -(\sin\vartheta_1)\frac{\partial}{\partial\varphi}\left[\varepsilon_{T1s} - W(\varepsilon_{T1s}N) - \frac{\sigma_1^2}{2!}\frac{\partial^2 W(\varepsilon_{T1}N)}{\partial\delta_1^2}(\delta_1 = 0) + \ldots\right] - Str\frac{\partial\varepsilon_{T1s}}{\partial t_1}\sin\vartheta_1. \quad (55)$$

The function $I(\varepsilon_{T1}N)$ assumes the form:

$$I(\varepsilon_{T1}N) = J(\varepsilon_{T1s}N) + \frac{\sigma_1^2}{2!}\left(\frac{\partial^2 J(\varepsilon_{T1}N)}{\partial\delta_1^2}\right)_{\delta_1=0} + \ldots, \quad (56)$$

where:

$$\left(\frac{\partial^2 J(\varepsilon_{T1}N)}{\partial\delta_1^2}\right)_{\delta_1=0} = \left(\frac{\partial^2 W(\varepsilon_{T1}N)}{\partial\delta_1^2}\right)_{\delta_1=0} Y(\varepsilon_{T1s}N) + 2\left(\frac{\partial W(\varepsilon_{T1}N)}{\partial\delta_1}\right)_{\delta_1=0}\left(\frac{\partial Y(\varepsilon_{T1}N)}{\partial\delta_1}\right)_{\delta_1=0}$$
$$+\left(\frac{\partial^2 Y(\varepsilon_{T1}N)}{\partial\delta_1^2}\right)_{\delta_1=0} W(\varepsilon_{T1s}N) - \left(\frac{\partial Y(\varepsilon_{T1}N)}{\partial\delta_1}\right)_{\delta_1=0} \quad (57)$$

and

$$\left(\frac{\partial W(\varepsilon_{T1}N)}{\partial\delta_1}\right)_{\delta_1=0} = 1 - W^*(\varepsilon_{T1s}N)W(\varepsilon_{T1s}N), \quad (58)$$

$$W(\varepsilon_{T1s}N) \equiv \frac{\int_0^{\varepsilon_{T1s}}\left(\int_0^{Nr_1} e^{-\chi_1^2}d\chi_1\right)dr_1}{\int_0^{N\varepsilon_{T1s}} e^{-\chi_1^2}d\chi_1}, \quad W^*(\varepsilon_{T1s}N) \equiv \frac{N\exp(-N^2\varepsilon_{T1s}^2)}{\int_0^{N\varepsilon_{T1s}} e^{-\chi_1^2}d\chi_1}, \quad (59)$$

$$\left(\frac{\partial^2 W(\varepsilon_{T1}N)}{\partial\delta_1^2}\right)_{\delta_1=0} = -W^*(\varepsilon_{T1s}N) + 2[N^2\varepsilon_{T1s} + W^*(\varepsilon_{T1s}N)]W^*(\varepsilon_{T1s}N)W(\varepsilon_{T1s}N), \quad (60)$$

$$Y(\varepsilon_{T1s}N)=\frac{2}{\sqrt{\pi}}\int_0^{\varepsilon_{T1s}N}\left(e^{\chi_1^2}\int_0^{\chi_1}e^{-\chi_2^2}d\chi_2\right)d\chi_1-\frac{2}{\sqrt{\pi}}\int_0^{\varepsilon_{T1s}N}e^{-\chi_1^2}d\chi_1\int_0^{\varepsilon_{T1s}N}e^{\chi_1^2}d\chi_1, \tag{61}$$

$$\left(\frac{\partial Y(\varepsilon_{T1}N)}{\partial\delta_1}\right)_{\delta_1=0}=\frac{-2N}{\sqrt{\pi}}e^{-N^2\varepsilon_{T1s}^2}\int_0^{\varepsilon_{T1s}N}e^{\chi_1^2}d\chi_1, \tag{62}$$

$$\left(\frac{\partial^2 Y(\varepsilon_{T1}N)}{\partial\delta_1^2}\right)_{\delta_1=0}=\frac{-2N^2}{\sqrt{\pi}}+\frac{4N^3}{\sqrt{\pi}}\varepsilon_{T1s}e^{-N^2\varepsilon_{T1s}^2}\int_0^{\varepsilon_{T1s}N}e^{\chi_1^2}d\chi_1. \tag{63}$$

The time-dependent gap height with perturbations and stochastic changes can be represented by the following equation:

$$\varepsilon_{T1}=\varepsilon_{T1s}(\varphi,\ \vartheta_1,\ t_1)+\delta_1=\varepsilon_{T1s}(\varphi,\ \vartheta_1)\ [1+s_1\exp(-t_0t_1\omega_0)]+\delta_1. \tag{64}$$

The time-independent value of the smooth part of the gap-height can be expressed in a dimensional form:

$$\varepsilon_0\ \varepsilon_{T1s}(\varphi,\ \vartheta_1)=\varepsilon_{Ts}(\varphi,\ \vartheta_1)\equiv\Delta\varepsilon_1\cos\varphi\sin\vartheta_1+\Delta\varepsilon_2\sin\varphi\sin\vartheta_1-\Delta\varepsilon_3\cos\vartheta_1-R$$

$$+\left[(\Delta\varepsilon_1\cos\varphi\sin\vartheta_1+\Delta\varepsilon_2\sin\varphi\sin\vartheta_1-\Delta\varepsilon_3\cos\vartheta_1)^2+(R+\varepsilon_{\min})(R+2D+\varepsilon_{\min})\right]^{0.5}. \tag{65}$$

We assume the centre of spherical bone head to be in the point $O(0,0,0)$ and the centre of spherical cartilage in the point $O_1(x-\Delta\varepsilon_1,\ y-\Delta\varepsilon_2,\ z+\Delta\varepsilon_3)$. The eccentricity has the value of D (see figure 2).

The dimensionless function $s_1=s(\varphi,\ \vartheta_{1s})/\varepsilon_{Ts}(\varphi,\ \vartheta_1)$ at $\vartheta_{1s}\equiv\vartheta_s/R$, $\vartheta_1\equiv\vartheta/R$ describes the changes in the gap height during the impulsive motion caused by the force P. The gap height increases if $s_1>0$ and decreases if $s_1<0$. The symbol ω_0 stands for an angular velocity in s^{-1} and describes the time-varying perturbations in unsteady flow of synovial fluid in joint gap in the height direction. If t_1 increases, then an enlarged gap-height decreases at $s_1>0$, and in a sufficiently long time after impulse it attains the same, time-independent value ε_{Ts}. If dimensionless time t_1 decreases, then the reduced gap-height increases at $s_1<0$. In sufficiently long time after impulse, the gap attains the same time-independent value ε_{Ts} (figure 2).

If t_1 tends to infinity, i.e. N tends to zero, then equation (55) tends to a classical Reynolds equation, provided that the conditions are random. To explain this fact we calculate the following limits:

$$\lim_{N\to0}\frac{\sqrt{\pi}}{2N^2}Y(\chi=\varepsilon_{T1s}N)\equiv\lim_{N\to0}\frac{\sqrt{\pi}}{2N^2}\left[\int_0^{\varepsilon_{T1s}N}\exp(\chi^2)\mathrm{erf}(\chi)d\chi-\mathrm{erf}(\varepsilon_1N)\int_0^{\varepsilon_{T1s}N}\exp(\chi^2)d\chi\right]$$

$$=\lim_{N\to0}\frac{1}{N^2}\left\{\int_0^{\varepsilon_{T1s}N}\left[\exp(\chi^2)\int_0^{\chi}\exp(-\chi_1^2)d\chi_1\right]d\chi-\left(\int_0^{\varepsilon_{T1s}N}\exp(-\chi^2)d\chi\right)\left(\int_0^{\varepsilon_{T1s}N}\exp(\chi^2)d\chi\right)\right\}$$

$$\overset{H}{=} -\lim_{N\to 0}\frac{\varepsilon_{T1s}\int_0^{N\varepsilon_{T1s}}\exp(\chi_1^2)d\chi_1}{2N\exp(\varepsilon_{T1s}^2N^2)} \overset{H}{=} -\frac{\varepsilon_{T1s}^2}{2}\lim_{N\to 0}\frac{\exp(\varepsilon_{T1s}^2N^2)}{\exp(\varepsilon_{T1s}^2N^2)+2\varepsilon_{T1s}^2N^2\exp(\varepsilon_{T1s}^2N^2)} = -\frac{\varepsilon_{T1s}^2}{2}. \quad (66)$$

The above limits are obtained after the Hospital rule application. If the following limits:

$$\lim_{N\to 0}\frac{\sqrt{\pi}}{2N^2}Y(\chi_1 = Nr_1) = -\frac{r_1^2}{2}, \quad \lim_{N\to 0}W(\varepsilon_{T1s}N) = \frac{\varepsilon_{T1s}}{2}, \quad (67)$$

and the other limits presented in Appendix 4 are taken into account, then equation (55) at $N \to 0$ tends to the following form:

$$\frac{1}{\sin\vartheta_1}\frac{\partial}{\partial\varphi}\left\{\left[\left(-\frac{\varepsilon_{T1s}^2}{2}\right)\frac{\varepsilon_{T1s}}{2}-\int_0^{\varepsilon_{T1s}}\left(-\frac{r_1^2}{2}\right)dr_1+\frac{\sigma_1^2}{2!}\left(\frac{\varepsilon_{T1s}^2}{2}\times 0-2\varepsilon_{T1s}\times\frac{1}{2}+\frac{\varepsilon_{T1s}}{2}(-1)-(-\varepsilon_{T1s})\right)\right]\frac{\partial p_{10}}{\partial\varphi}\right\}$$

$$+\frac{\partial}{\partial\vartheta_1}\left\{\left[\left(-\frac{\varepsilon_{T1s}^2}{2}\right)\frac{\varepsilon_{T1s}}{2}-\int_0^{\varepsilon_{T1s}}\left(-\frac{r_1^2}{2}\right)dr_1+\frac{\sigma_1^2}{2!}\left(\frac{\varepsilon_{T1s}^2}{2}\times 0-2\varepsilon_{T1s}\times\frac{1}{2}+\frac{\varepsilon_{T1s}}{2}(-1)-(-\varepsilon_{T1s})\right)\right]\frac{\partial p_{10}}{\partial\vartheta_1}\sin\vartheta_1\right\}$$

$$= -(\sin\vartheta_1)\frac{\partial}{\partial\varphi}\left[\int_0^{\varepsilon_{T1}}\left(1-\frac{r_1}{\varepsilon_{T1s}}\right)dr_1+\frac{\sigma_1^2}{2!}\times 0\right]-\frac{\partial(\varepsilon_{T1s})}{\partial t_1}\sin\vartheta_1. \quad (68)$$

After final calculations, we obtain the following form of the classical Reynolds equation in the spherical coordinates but in random conditions:

$$\frac{1}{\sin\vartheta_1}\frac{\partial}{\partial\varphi}\left[(\varepsilon_{T1s}^3+3\sigma_1^2\varepsilon_{T1s})\frac{\partial p_{10}}{\partial\varphi}\right]+\frac{\partial}{\partial\vartheta_1}\left[(\varepsilon_{T1s}^3+3\sigma_1^2\varepsilon_{T1s})\frac{\partial p_{10}}{\partial\vartheta_1}\sin\vartheta_1\right] = 6\frac{\partial\varepsilon_{T1s}}{\partial\varphi}\sin\vartheta_1, \quad (69)$$

where $0 \le \varphi < 2\pi\theta_1$, $0 \le \theta_1 < 1$, $\pi/8 \le \vartheta_1 \le \pi/2$.

Equation (69) determines a time-independent pressure function with stochastic changes. If the standard deviation tends to zero ($\sigma_1 \to 0$), then equation (69) tends to the classical Reynolds equation for stationary flow without random conditions.

7. Numerical calculations

In the case of impulsive motion, the dimensionless pressure p_{10} and its dimensionless corrections p_{11}, p_{12}, … in the lubrication region Ω $\{0 \le \varphi < \pi, \pi/8 \le \vartheta_1 \le \pi/2\}$ are determined. The pressure p_{10} is determined by virtue of the modified Reynolds equations (48), (55) by taking into account the gap height (64), (65). Numerical calculations are performed for [22]: the radius of spherical bone head R = 0.0265 m, the angular velocity of the impulsive perturbations of acetabulum ω_0 = 0.4 s^{-1}, a characteristic dimensional time t_0 = 0.000001 s. The gap height (64), (65) is

taken into

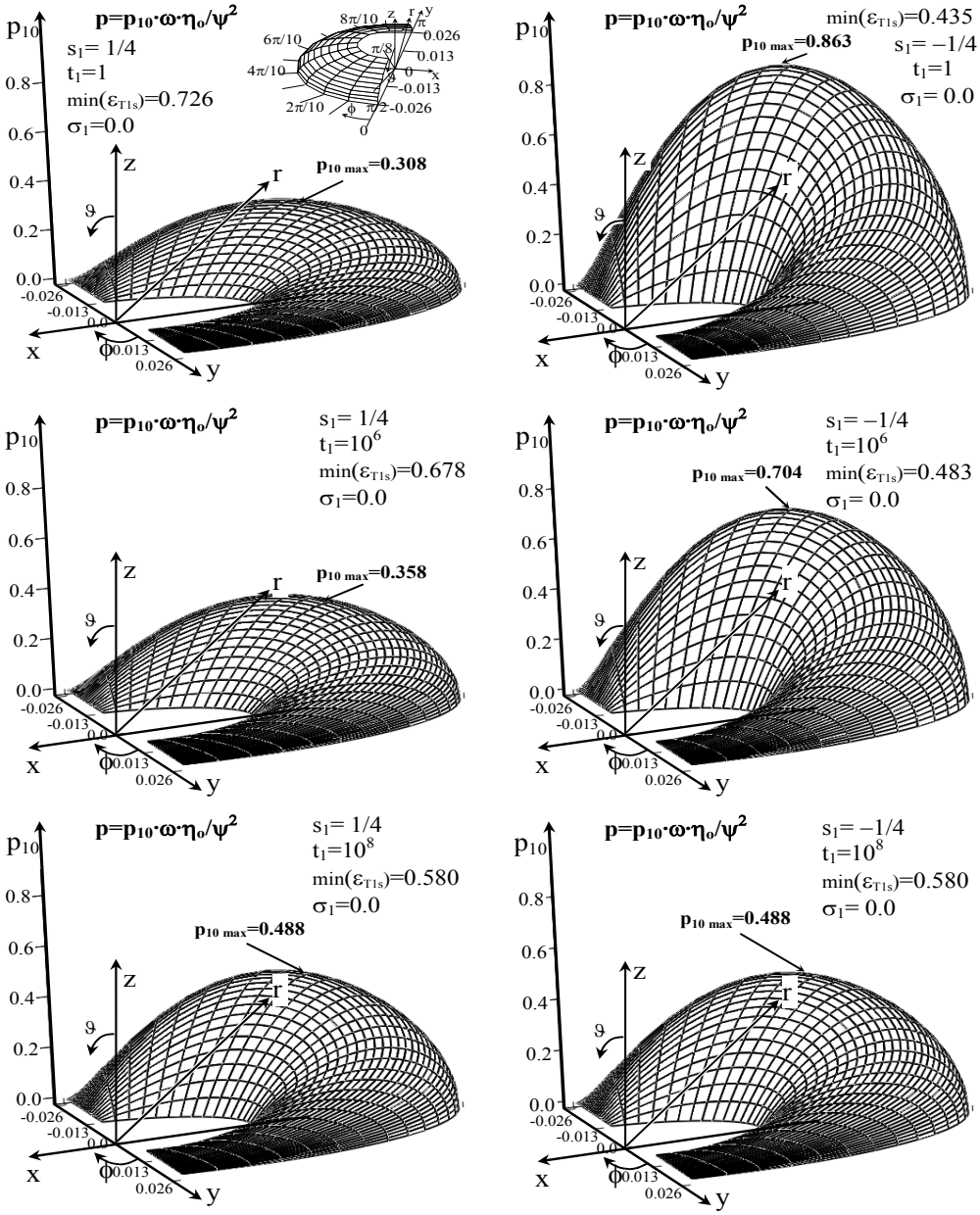

Fig. 5. Dimensionless hydrodynamic pressure distributions inside the gap of human spherical hip joint in the region Ω: $0 \le \varphi \le \pi$, $\pi R/8 \le \vartheta \le \pi R/2$ without stochastic changes ($\sigma_1 = 0$) in the dimensionless time: $t_1 = 1$ (i.e. $t = 0.000\,001$ s), $t_1 = 1000\,000$ (i.e. $t = 1$ s), $t_1 = 100\,000\,000$ (i.e. $t = 100$ s) after the impulse occurrence for the increasing (decreasing) effects of gap-height changes (the right (left) columns of the figures, respectively). The results are obtained at the following data:

$R = 0.0265$ m; $\eta_0 = 0.60$ Pas; $\rho = 1010$ kg/m^3; $\varepsilon_0 = 10$ μm, $\Delta\varepsilon_1 = 4$ μm; $\Delta\varepsilon_2 = 0.5$ μm; $\Delta\varepsilon_3 = 3$ μm; $\psi \equiv \varepsilon_0/R = 3.8\cdot10^{-4}$; $\omega = 1.0$ s^{-1}; $\omega_0 = 0.4$ s^{-1}; $Str = 1\,000\,000$; $Re\cdot Str = 0.168$; $De\cdot Str = 0.833$

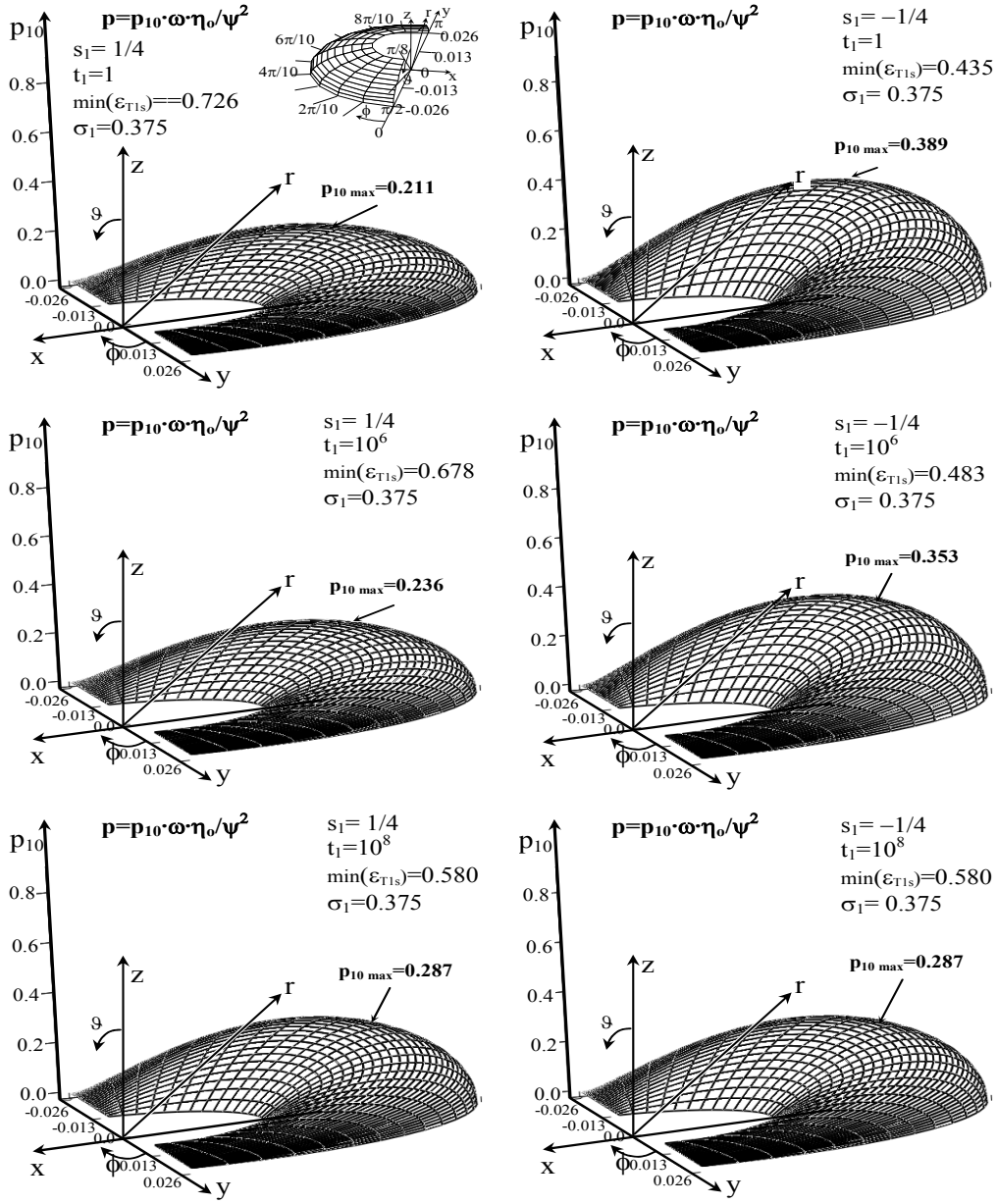

Fig. 6. Dimensionless hydrodynamic pressure distributions inside the gap of human spherical hip joint in the region Ω: $0 \le \varphi \le \pi$, $\pi R/8 \le \vartheta \le \pi R/2$ for stochastic changes at the standard deviation $\sigma_1 = 0.375$ (i.e. 0.37 μm) in the dimensionless time: $t_1 = 1$ (i.e. $t = 0.000\,001$ s), $t_1 = 1000\,000$ (i.e. $t = 1$ s), $t_1 = 100\,000\,000$ (i.e. $t = 100$ s) after the impulse occurrence for the increasing (decreasing) effects of gap-height changes (the right (left) columns of the figures, respectively). The results are obtained for the

following data: $R = 0.0265$ m; $\eta_0 = 0.60$ Pas; $\rho = 1010$ kg/m^3; $\varepsilon_0 = 10$ μm, $\Delta\varepsilon_1 = 4$ μm; $\Delta\varepsilon_2 = 0.5$ μm; $\Delta\varepsilon_3 = 3$ μm; $\psi \equiv \varepsilon/R \approx 3.8 \cdot 10^{-4}$; $\omega = 1.0$ s^{-1}; $\omega_0 = 0.4$ s^{-1}; $Str = 1\,000\,000$; $Re \cdot Str = 0.168$; $De \cdot Str = 0.833$

account, where such eccentricities of bone head as $\Delta\varepsilon_1 = 4.0$ μm, $\Delta\varepsilon_2 = 0.5$ μm, $\Delta\varepsilon_3 = 3$ μm are assumed. In the calculations, we take the optimal dimensionless standard deviation $\sigma_1 = 0.375$. We assume that the dynamic viscosity of synovial fluid η_0 is 0.60 Pas, a pseudo-viscosity coefficient $\beta = 0.000\,0005$ Pas^2, the density of synovial fluid $\rho = 1010$ kg/m^3, the angular velocity of spherical bone head $\omega = 1.0$ s^{-1}, the minimum value of gap height $\min(\varepsilon_{T1s})$ changes within the time interval of $0.000001 \text{ s} \le t \le 100$ s and attains the values within the range from 0.435 (4.3 μm) to 0.726 (18.2 μm). An average relative radial clearance $\psi \equiv \varepsilon_0/R = 3.8 \cdot 10^{-4}$. The characteristic dimensional pressure $p_0 = \omega\eta_0/\psi^2$ reaches the value of 4.2135 MPa. A characteristic dimensional gap height $\varepsilon_0 = 10$ microns and the Strouhal number $Str = 10^6$, $Re \cdot Str = 0.168$, $De \cdot Str = 0.833$. In this case, we have $0 \le \beta/\eta_0 t < 1$. For the dimensionless times: $t_1 = 1$, $t_1 = 1000$, $t_1 = 100\,000$, $t_1 = 1000\,000$, $t_1 = 10\,000\,000$, $t_1 = 100\,000\,000$, i.e. for dimensional times: $t = 0.000\,001$ s; $t = 0.001$ s; $t = 0.1$ s; $t = 1.0$ s; $t = 10.0$ s; $t = 100.0$ s, respectively, and for $s_1 = \pm 0.25$ we obtain the distributions of dimensionless pressure (figures 5 and 6). To obtain real values of time, we must multiply the dimensionless values t_1 by a characteristic time value $t_0 = 0.000001$ s, for example, $t_1 = 1000\,000$ denotes 1 s after an impulse. To obtain a dimensional value of pressure, we must multiply the dimensionless values of pressure (see figures 5 and 6) by

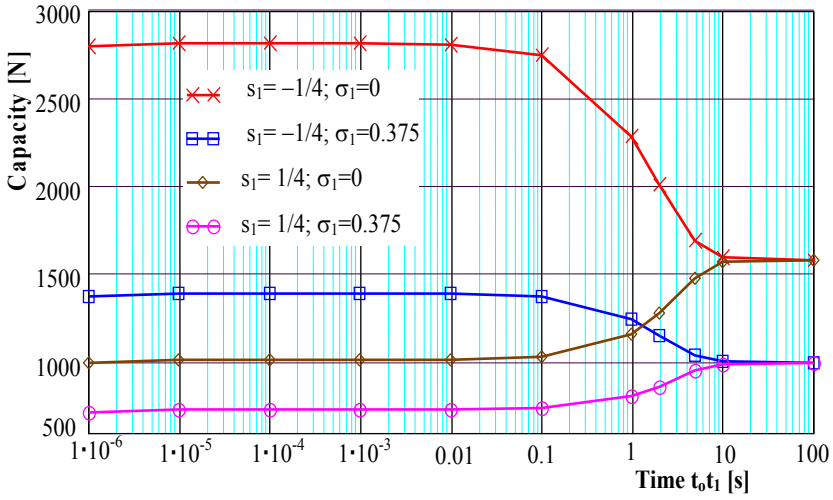

Fig. 7. Dimensional values of capacity versus dimensional time in the range from 10^{-6} second to 100 seconds after impulse inside the gap of human spherical hip joint in the region Ω: $0 \le \varphi \le \pi$, $\pi R/8 \le \vartheta \le \pi R/2$ for stochastic changes of roughness of cartilage surface at the standard deviation $\sigma_1 = 0.375$ (i.e. 0.37 μm) and without random effects at $\sigma_1 = 0$. The results are obtained for the following data: $R = 0.0265$ m; $\eta_0 = 0.60$ Pas; $\rho = 1010$ kg/m^3; $\varepsilon_0 = 10$ μm; $\Delta\varepsilon_1 = 4$ μm; $\Delta\varepsilon_2 = 0.5$ μm;

$\Delta\varepsilon_3 = 3$ μm; $\psi \equiv \varepsilon_0/R = 3.8\cdot10^{-4}$; $\omega = 1.0$ s^{-1}; $\omega_0 = 0.4$ s^{-1}; $t_0 = 0.000\,001$ s; $Str = 1\,000\,000$; $Re\cdot Str = 0.168$; $De\cdot Str = 0.833$

a characteristic value of pressure p_0. Figure 5 presents the dimensionless values of pressure without random effects at $\sigma_1 = 0$. Dimensionless values of pressure given in figure 6 are obtained for stochastic changes of gap height at $\sigma_1 = 0.375$. The distributions of dimensionless pressure at $s_1 > 0$ presented on the right-hand side of figures 5 and 6 are obtained for an enlargement effect of gap height caused by impulsive motion. If in this case the time after an impulse lenghtens, the gap height decreases and pressure increases, and in a sufficiently long time after impulse the latter tends to the time-independent pressure. The pressure distributions presented for $s_1 < 0$ on the left-hand side in figures 5 and 6 are obtained for the limited effects of gap height caused by impulsive motion. If in this case the time after the impulse is lenghtened, the gap increases and the pressure decreases, and in a sufficiently long time after impulse the latter tends to the time-independent pressure. Figure 7 presents the dimensional value of capacity versus the dimensional time ranging from the beginning of the impulse to 100 seconds after the impulse.

8. Conclusions

- If the trauma is responsible for an increase in the gap height ($s_1 > 0$) of a normal joint, then in the time just after impulse the gap height decreases and the pressure increases. In a sufficiently long time after impulse, the gap-height and the pressure attain time-independent values.

If the trauma is responsible for a decrease in the gap height ($s_1 < 0$), then in the time after impulse the gap height increases and the pressure decreases. In a sufficiently long time after impulse, the gap height and the pressure attain time-independent values.

- If the time after the impulse occurrence is long enough, i.e. $t_1 \to \infty$, and if we take the optimal standard deviations of gap height, then the pressure distributions tend to the identical pressure distributions for the increasing ($s_1 > 0$) and decreasing ($s_1 < 0$) effects of the gap height changes caused by the impulse. This limit pressure distribution can also be obtained based on the classical Reynolds equation (67) for $\sigma_1 = 0$.
- From the numerical calculations we conclude that the pressure and capacity of the joint obtained at the optimal standard deviation $\sigma_1 = 0.375$ by virtue of the measurements of normal cartilage surfaces of the human hip joint decrease by about 30% in comparison with the pressure and capacity obtained for smooth cartilage surface without asperities and random effects.

• The numerical calculations show that the biggest changes of pressure distribution and capacity in human joint occur within the time interval from 0.1 to 10 seconds after impulse.

Acknowledgement

This paper was supported by the State Committe for Scientific Research in years 2003–2006 as Scientific Project KBN 411E-030-25 and by Project ToK-2004-2008-MTkD-CT-517226.

Author thanks for cooperation with Central Institute Department of Biomedical Engineering at University of Ulm in Germany and cooperation with the Forschungszentrum Karlsruhe Institut für Biologische Gränzflächen.

Appendix 1

The probability density functions (12) have the forms:

$$f_1(\delta_1) \equiv \begin{cases} \dfrac{3}{4c_{11}}\left(1-\dfrac{\delta_1^2}{c_{11}^2}\right) & \text{for } -c_{11} \le \delta_1 \le +c_{11}, \\ 0 & \text{for } |\delta_1| > c_{11}, \end{cases} \quad f_3(\delta_1) \equiv \begin{cases} \dfrac{35}{32c_{31}}\left(1-\dfrac{\delta_1^2}{c_{31}^2}\right)^3 & \text{for } -c_{31} \le \delta_1 \le +c_{31}, \\ 0 & \text{for } |\delta_1| > c_{31}, \end{cases}$$

$$f_5(\delta_1) \equiv \begin{cases} \dfrac{693}{512c_{51}}\left(1-\dfrac{\delta_1^2}{c_{51}^2}\right)^5 & \text{for } -c_{51} \le \delta_1 \le +c_{51}, \\ 0 & \text{for } |\delta_1| > c_{51}, \end{cases} \quad f_7(\delta_1) \equiv \begin{cases} \dfrac{6435}{4096c_{71}}\left(1-\dfrac{\delta_1^2}{c_{71}^2}\right)^7 & \text{for } -c_{71} \le \delta_1 \le +c_{71}, \\ 0 & \text{for } |\delta_1| > c_{71}, \end{cases}$$

$$f_k(\delta_1) \equiv \begin{cases} \left(1-\dfrac{\delta_1^2}{c_{k1}^2}\right)^k \left(\displaystyle\int_{-c_{k1}}^{c_{k1}} \left(1-\dfrac{\delta_1^2}{c_{k1}^2}\right)^k d\delta_1 \right)^{-1} & \text{for } -c_{k1} \le \delta_1 \le +c_{k1}, \\ 0 & \text{for } |\delta_1| > c_{k1}. \end{cases} \tag{A1.1}$$

The function of the order k presented in (A1.1) for $k = 1, 3, 5, \ldots$ can be given in the form:

$$f_k(\delta_1) \equiv \begin{cases} \sqrt{\dfrac{k}{\pi}}\left(1-\dfrac{\delta_1^2}{c_{k1}^2}\right)^k \left[c_{k1} \displaystyle\int_{-1}^{1} \sqrt{\dfrac{k}{\pi}}(1-y_1)^k dy_1 \right]^{-1} & \text{for } -c_{k1} \le \delta_1 \le +c_{k1}, -1 \le y_1 \le +1, \\ 0 & \text{for } |\delta_1| > c_{k1}. \end{cases} \tag{A1.2}$$

From equations (13), (16), (17) it follows [14]:

$$c_{k1} \ge m_{k1} \equiv \sqrt{\frac{k}{\pi}} \left(\int_{-1}^{1} \sqrt{\frac{k}{\pi}}(1-y_1)^k dy_1 \right)^{-1} \quad \text{for } -c_{k1} \le \delta_1 \le +c_{k1}, -1 \le y_1 \le +1, \tag{A1.3}$$

where:

$$\lim_{k\to\infty} \left\{ \int_{-1}^{1} \left[\sqrt{\frac{k}{\pi}}(1-y_1)^k \right] dy_1 \right\} = \int_{-1}^{1} \left\{ \lim_{k\to\infty} \left[\sqrt{\frac{k}{\pi}}(1-y_1)^k \right] \right\} dy_1 = \int_{-1}^{1} D(y_1) dy_1 = \int_{-\infty}^{\infty} D(\delta_1) d\delta_1 = 1 \tag{A1.4}$$

and D denotes the Dirac function.

We insert (A1.3) into (A1.2), hence if k tends to infinity, we obtain:

$$f_{\infty}(\delta_1) = \lim_{k\to\infty}\left(1-\frac{\delta_1^2}{c_{k1}^2}\right)^k. \tag{A1.5}$$

A new variable $K \equiv c_{k1}/\delta_1$ tends to infinity, if k tends to infinity. Hence by using the result (A1.3), we arrive at the limit (A1.5) in the following form:

$$f_{\infty}(\delta_1) = \left[\lim_{K\to\infty}\left(1-\frac{1}{K^2}\right)^{K^2}\right]^{\frac{\delta_1^2}{c_{k1}^2}k} = \left(\frac{1}{e}\right)^{\pi\delta_1^2} = e^{-\pi\delta_1^2}. \tag{A1.6}$$

By using a new variable x_1, the cumulative function in infinity obtains the form:

$$\int_{-\infty}^{+\infty} f_{\infty}(\delta_1)\,d\delta_1 = \int_{-\infty}^{+\infty} e^{-\pi\delta_1^2}\,d\delta_1 = \frac{1}{\sqrt{\pi}}\int_{-\infty}^{+\infty} e^{-x_1^2}\,dx_1 = 1 \quad \text{for} \quad x_1 \equiv \delta_1\sqrt{\pi}. \tag{A1.7}$$

Appendix 2

• The first proof. If k tends to infinity, then by virtue of limit (A1.6) and formulae (19)–(21) the boundary value of standard deviation has the form:

$$\sigma_{\infty 1} = \sqrt{\int_{-\infty}^{\infty}\delta_1^2 e^{-\pi\delta_1^2}\,d\delta_1}. \tag{A2.1}$$

Its integration by parts gives:

$$\int_{-\infty}^{\infty}\delta_1^2 e^{-\pi\delta_1^2}\,d\delta_1 = -\frac{1}{2\pi}\left(2\lim_{\delta_1\to\infty}\frac{\delta_1}{e^{\pi\delta_1^2}}\right) + \frac{1}{2\pi}\int_{-\infty}^{\infty} e^{-\pi\delta_1^2}\,d\delta_1 = \frac{1}{2\pi}\int_{-\infty}^{\infty} e^{-\pi\delta_1^2}\,d\delta_1. \tag{A2.2}$$

Using the new variable x_1 in integrals (A2.2), we obtain:

$$\int_{-\infty}^{\infty}\delta_1^2 e^{-\pi\delta_1^2}\,d\delta_1 = \frac{1}{2\pi}\int_{-\infty}^{\infty} e^{-\pi\delta_1^2}\,d\delta_1 = \frac{1}{2\pi}\frac{1}{\sqrt{\pi}}\int_{-\infty}^{\infty} e^{-x_1^2}\,dx_1 = \frac{1}{2\pi}. \tag{A2.3}$$

By using expression (A2.3), the boundary value of standard deviation (A2.1) has the form:

$$\sigma_{\infty 1} = \frac{1}{\sqrt{2\pi}} = 0.4418\ldots \tag{A2.4}$$

• The second proof. We insert the result (16) into (22), and (22) into (19). Hence we obtain the standard deviation in the following form:

$$\sigma_{k1} = c_{k1}\sqrt{\frac{\int_{-1}^{+1} y_1^2(1-y_1^2)^k\,dy_1}{\int_{-1}^{+1}(1-y_1^2)^k\,dy_1}} \quad \text{for} \quad k = 1, 3, 5, 7, ... \tag{A2.5}$$

After simple mapping we have:

$$\sigma_{k1} = c_{k1}\sqrt{1-\sqrt{\frac{k}{k+1}}\frac{\int_{-1}^{+1}\sqrt{\frac{k+1}{\pi}}(1-y_1^2)^{k+1}\,dy_1}{\int_{-1}^{+1}\sqrt{\frac{k}{\pi}}(1-y_1^2)^k\,dy_1}} \quad \text{for} \quad k = 1, 3, 5, 7, ... \tag{A2.6}$$

By virtue of (A1.3), (A1.4) we can write the formula (A2.6) in the following form:

$$\sigma_{\infty 1} = \lim_{k\to\infty}\sqrt{\frac{k}{\pi}}\sqrt{1-\sqrt{\frac{k}{k+1}}} = \frac{1}{\sqrt{2\pi}} \quad \text{for} \quad k = 1, 3, 5, 7, ... \tag{A2.7}$$

The limit (A2.7) is obtained after the Hospital rule application.

Appendix 3

The general solutions of ordinary differential equations (36) for $i = \varphi, \vartheta$ have the form:

$$v_{i0\Sigma}(\chi) = C_{i1}v_{01}(\chi) + C_{i2} + v_{i03}(\chi) \quad \text{for} \quad i = \varphi, \vartheta, \tag{A3.1}$$

where C_{i1}, C_{i2} are integral constants. The particular solutions of homogeneous and nonhomogeneous differential equations are as follows:

$$v_{01}(\chi) = \int_0^{\chi} e^{-\chi_1^2}\,d\chi_1, \quad v_{02}(\chi) = 1, \tag{A3.2}$$

$$v_{i03}(\chi) = -\frac{1}{N_i^2}\frac{\partial p_{10}}{\partial \alpha_i}\left[\int_0^{\chi} e^{\chi_1^2}v_{01}(\chi_1)d\chi_1 - v_{01}(\chi)\int_0^{\chi} e^{\chi_1^2}\,d\chi_1\right], \tag{A3.3}$$

where $0 \le \chi_1 \le \chi \equiv r_1 N$. If $t_1 \to 0$, then $N \to \infty$, thus $\chi \to \infty$. If $t_1 \to \infty$, then N$\to$0. Hence for $r_1 > 0$ we have $\chi \to 0$. For $t_1 > 0$ and $r_1 = 0$ we have $\chi = 0$. The following limits are true:

$v_{01}(\chi) = \pi^{0.5}/2$ for $\chi \to \infty$, $t_1 \to 0$, $N \to \infty$; $v_{01}(\chi) = 0$, for $\chi \to 0$, $r_1 = 0$, $0 < t_1 < t_2 < \infty$, $N > 0$;

$v_{i03}(\chi) = 0$ for $\chi \to 0$, $r_1 = 0$, $0 < t_1 < t_2 < \infty$, $N > 0$, $i = \varphi, \vartheta$;

$$v_{01}(\chi) = 0 \quad \text{for } \chi \to 0,\ r_1 > 0,\ t_1 \to \infty,\ N \to 0; \tag{A3.4}$$

$$v_{\varphi 03}(\chi) = -\frac{r_1^2}{2\sin\vartheta_1}\frac{\partial p_{10}}{\partial \varphi} \quad \text{for} \quad \chi \to 0, r_1 > 0, t_1 \to \infty, N \to 0;$$

$$v_{\vartheta 03}(\chi) = -\frac{r_1^2}{2}\frac{\partial p_{10}}{\partial \vartheta_1} \quad \text{for} \quad \chi \to 0, r_1 > 0, t_1 \to \infty, N \to 0. \tag{A3.5}$$

The spherical bone head moves in circumferential direction φ only. Hence the synovial fluid velocity components on the surface of bone head in circumferential direction are equal to the peripheral velocity of spherical surface of bone head. The synovial fluid velocity component on a spherical bone head surface in a meridional direction ϑ equals zero, because spherical bone head is motionless in the direction ϑ. Viscous synovial fluid flows around the bone head. Hence on its surface the synovial fluid velocity component in the gap-height direction equals zero.

Therefore we have the following boundary conditions:

$$v_{\varphi 0\Sigma}(\chi = 0) = \sin\vartheta_1, \quad v_{\vartheta 0\Sigma}(\chi = 0) = 0, \quad v_{r0\Sigma}(\chi = 0) = 0$$
$$\text{for } r_1 = 0 \Leftrightarrow \chi = 0 \quad \text{and} \quad 0 < t_1 < t_2 < \infty, \quad N > 0. \tag{A3.6}$$

The spherical acetabulum surface is motionless in circumferential and meridional directions. But spherical acetabulum has any vibrations in the gap-height direction. Hence the gap height changes with time. Thus synovial fluid velocity components on the acetabulum surface are equal to zero in circumferential and meridional directions. The synovial fluid velocity component in gap-height direction r is equal to the first derivative of the gap height with respect to the time. Hence we have the following boundary conditions:

$$v_{\varphi 0\Sigma}(\chi = M) = 0, \; v_{\vartheta 0\Sigma}(\chi = M) = 0, \; v_{r0\Sigma}(\chi = M) = Str\,\partial\varepsilon_{T1}/\partial t_1;$$
$$r_1 \to \varepsilon_1 \Leftrightarrow \chi \to N\varepsilon_{T1} \equiv M \text{ and } 0 < t_1 < t_2 < \infty, \; N > 0\,, \tag{A3.7}$$

where: $\varepsilon_T = \varepsilon_0 \varepsilon_{1T}$ – the gap height, ε_{T1} – the dimensionless total gap height, $Str \equiv 1/\omega t_0$.

Imposing conditions (A3.7), (A3.6) on the general solution (A3.3) we obtain:

$$\begin{aligned}
&C_{\varphi 1} v_{01}(\chi = 0) + C_{\varphi 2} + v_{\varphi 03}(\chi = 0) = \sin\vartheta_1 \quad \text{for } r_1 = 0,\\
&C_{\varphi 1} v_{01}(\chi = M) + C_{\varphi 2} + v_{\varphi 03}(\chi = M) = 0 \quad \text{for } r_1 = \varepsilon_{T1},\\
&C_{\vartheta 1} v_{01}(\chi = 0) + C_{\vartheta 2} + v_{\vartheta 03}(\chi = 0) = 0 \quad \text{for } r_1 = 0,\\
&C_{\vartheta 1} v_{01}(\chi = M) + C_{\vartheta 2} + v_{\vartheta 03}(\chi = M) = 0 \quad \text{for } r_1 = \varepsilon_{T1}.
\end{aligned} \tag{A3.8}$$

Taking into account limits (A3.4), (A3.5), the system of equations (A3.8) has the following solutions:

$$C_{\varphi 1} = -\frac{\sin\vartheta_1 + v_{\varphi 03}(M)}{v_{01}(M)}, \quad C_{\vartheta 1} = -\frac{v_{\vartheta 03}(M)}{v_{01}}, \quad C_{\varphi 2} = \sin\vartheta_1, \quad C_{\vartheta 2} = 0. \tag{A3.9}$$

Appendix 4

We calculate the following limits:

$$\lim_{N\to 0} W^*(\varepsilon_{T1s} N) \equiv \lim_{N\to 0} \frac{N\exp(-N^2\varepsilon_{T1s}^2)}{\int_0^{\varepsilon_{T1s}} e^{-\chi_1^2} d\chi_1} = \lim_{N\to 0} \frac{\exp(-N^2\varepsilon_{T1s}^2) - 2N^2\varepsilon_{T1s}^2\exp(-N^2\varepsilon_{T1s}^2)}{\varepsilon_{T1}\exp(-N^2\varepsilon_{T1s}^2)} = \frac{1}{\varepsilon_{T1s}}, \tag{A4.1}$$

$$\lim_{N\to 0}\left(\frac{\partial^2 W(\varepsilon_{T1}N)}{\partial\delta_1^2}\right)_{\delta_1=0} = -\lim_{N\to 0}W^*(\varepsilon_{T1s}N)+2\lim_{N\to 0}\left[N^2\varepsilon_{T1s}+W^*(\varepsilon_{T1s}N)\right]W^*(\varepsilon_{T1s}N)W(\varepsilon_{T1s}N)$$

$$= -\frac{1}{\varepsilon_{T1s}}+2\left(0+\frac{1}{\varepsilon_{T1s}}\right)\frac{1}{\varepsilon_{T1s}}\frac{\varepsilon_{T1s}}{2}=0, \tag{A4.2}$$

$$\lim_{N\to 0}\left(\frac{\partial W(\varepsilon_{T1}N)}{\partial\delta_1}\right)_{\delta_1=0} = 1-\lim_{N\to 0}W^*(\varepsilon_{T1s}N)\lim_{N\to 0}W(\varepsilon_{T1s}N)=1-\frac{1}{\varepsilon_{T1s}}\frac{\varepsilon_{T1s}}{2}=\frac{1}{2}, \tag{A4.3}$$

$$2\lim_{N\to 0}\frac{\sqrt{\pi}}{2N^2}\left(\frac{\partial Y(\varepsilon_{T1}N)}{\partial\delta_1}\right)_{\delta_1=0} = \lim_{N\to 0}2\frac{\sqrt{\pi}}{2N^2}\left(\frac{-2N}{\sqrt{\pi}}\right)e^{-N^2\varepsilon_{T1s}^2}\int_0^{\varepsilon_{T1s}N}e^{\chi_1^2}d\chi_1$$

$$= -2\lim_{N\to 0}\left(-2N\varepsilon_{T1s}^2\int_0^{\varepsilon_{T1s}N}e^{\chi_1^2}d\chi_1+\varepsilon_{T1s}\right)=-2\varepsilon_{T1s}, \tag{A4.4}$$

$$\lim_{N\to 0}\frac{\sqrt{\pi}}{2N^2}\left(\frac{\partial^2 Y(\varepsilon_{T1}N)}{\partial\delta_1^2}\right)_{\delta_1=0} = -1+2\lim_{N\to 0}N\varepsilon_{T1s}e^{-N^2\varepsilon_{T1s}^2}\int_0^{\varepsilon_{T1s}N}e^{\chi_1^2}d\chi_1=-1, \tag{A4.5}$$

hence:

$$\frac{\sigma_1^2}{2!}\lim_{N\to 0}\frac{\sqrt{\pi}}{2N^2}\left(\frac{\partial^2 J(\varepsilon_{T1}N)}{\partial\delta_1^2}\right)_{\delta_1=0} = \frac{\sigma_1^2}{2!}\left[-\frac{\varepsilon_{T1s}^2}{2}\times 0-2\varepsilon_{T1s}\times\frac{1}{2}+\frac{\varepsilon_{T1s}}{2}\times(-1)-(-\varepsilon_{T1s})\right]=-\frac{\sigma_1^2}{4}\varepsilon_{T1s}. \tag{A4.6}$$

References

[1] BERNSTEIN B., *Hypo-elasticity and elasticity*, Arch. Ration. Mech. Anal., 1960, 6, pp. 90–104.

[2] DOWSON D., *Bio-Tribology of Natural and Replacement Synovial Joints*, [in:] Van Mow C., Ratcliffe A., Woo S.L-Y., *Biomechanics of Diarthrodial Joint*, Springer-Verlag, New York, Berlin, London, Paris, Tokyo, Hong Kong, 1990, Vol. 2, Chap. 29, pp. 305–345.

[3] EBERHARDT A.W., KEER L.M., LEWIS J.L., VITHOONTIEN V., *An analytical model of joint contact*, ASME J. Biomech. Eng., 1990, 112, pp. 407–413.

[4] FISZ M., *Rachunek prawdopodobieństwa i statystyka matematyczna*, PWN, Warszawa, 1969.

[5] FUNG Y.C., *Bioviscoelastic Solids*, [in:] *Biomechanics, Mechanical Properties of Living Tissues*, Berlin, Springer-Verlag, 1993.

[6] FUNG Y.C., *The Meaning of Constitutive Equations*, [in:] *Biomechanics, Mechanical Properties of Living Tissues*, Berlin, Springer-Verlag, 1993.

[7] FUNG Y.C., *Biomechanics: Mechanical Properties of Living Tissues*, Springer-Verlag, New York, 1993, pp. 220–241.

[8] FUNG C.A., *First course in continuum mechanics*: *for physical and biological engineers and scientists*, 3-rd ed., Englewood Cliffs, NJ, Prentice-Hall, 1993.

[9] FUNG C., *Biomechanics, Motion, Flow, Stress and Growth*, Springer-Verlag, New York, Hong Kong, 1993.

[10] GARCIA J.J., ALTIERO N.J., HAUT R.C., *Estimation of in Situ Elastic Properties of Biophasic Cartilage Based on a Transversely Isotropic Hypo-Elastic Model*, Journal of Biomechanical Engineering, February 2000, Vol. 122, pp. 1–8.

[11] HOLMES M.H., *Finite deformation of soft tissue: Analysis of a mixture model in uni-axial compression*, ASME J. Biomech. Eng., 1986, 108, pp. 372–381.

[12] JEMIOŁO S., TELEGA J.J., MICHALAK C., *Hyperelastic anisotropic model of soft tissues*, Acta Bioeng. Biomechanics, 2000, 2 Suppl. 1, pp. 235–240.
[13] JOHNSON G.A., RAJAGOPAL K.R.Y., WOO S.L., *A Single Integral Finite Strain (sifs) Model of Ligaments and Tendons*, Advances in Bioengineering, 1992, 22, pp. 245–248.
[14] KĄCKI E., *Równania różniczkowe cząstkowe w zagadnieniach fizyki i techniki*, WNT, Warszawa, 1989.
[15] KNOPP K., *Szeregi nieskończone*, PWN, 1956.
[16] MAUREL W., WU Y., THALMANN D., *Biomechanical Models for Soft Tissue Simulation*, Springer-Verlag, Berlin, Heidelberg, 1998.
[17] MOW V.C., HOLMES M.H., LAI, *Fluid transport and mechanical properties of articular cartilage*, Journal of Biomechanics, 1984, 17, pp. 337–394.
[18] MOW V.C., RATCLIFFE A., WOO S., *Biomechanics of Diarthrodial Joints*, Springer-Verlag, Berlin, Heidelberg, New York, 1990.
[19] MOW V.C., SOSLOWSKY L.J., *Friction, lubrication and wear of diarthrodial joints*, [in:] Mow V.C., Hayes W.C. (eds.), *Basic Orthopedic Biomechanics*, New York, Raven Press, 1991, pp. 254–291.
[20] MOW V.C., GUILAK F., *Cell Mechanics and Cellular Engineering*, Berlin, Heidelberg, New York, Springer-Verlag, 1994.
[21] NOWACKI W., *Teoria sprężystości*, PWN, Warszawa, 1970.
[22] RALSTON A., *A First Course in Numerical Analysis*, McGraw-Hill Co., New York, Toronto, London, Sydney, 1965.
[23] STEINHAGEN J., KURZ B., NIGGEMEYER O., BRUNS J., *The pathophysiology of cartilage diseases*, Ortopedia, Traumatologia, Rehabilitacja, 2001, Vol. 3, No. 2, pp. 163–168.
[24] SOBCZYK M., *Statystyka*, PWN, Warszawa, 1996.
[25] TEIPEL I., *The Impulsive Motion of a Flat Plate in a Viscoelastic Fluid*, Acta Mechanica, Springer-Verlag, 1981, 39, pp. 277–279.
[26] TRUESDELL C., *A First Course in Rational Continuum Mechanics*, Maryland, John Hopkins University, Baltimore, 1972.
[27] TRUESDELL C., *Hypo-elasticity*, J. Rational Mechanics and Analysis, 1955, 4, pp. 83–133.
[28] UNGETHÜM M., WINKLER-GNIEWEK W., *Tribologie in Medizin*, Tribologie Schmierungstechnik, 1990, 5, pp. 268–277.
[29] WIERZCHOLSKI K., PYTKO S., *Metoda wyznaczania parametrów biołożyska smarowanego cieczą nienewtonowską* (in Polish), Tribologia, 1993, 1, pp. 9–12.
[30] WIERZCHOLSKI K., PYTKO S., *Analytical calculations for experimental dependences between shear rate and synovial fluid viscosity*, Proc. of Internat. Tribology Conference, Japan, Yokohama, 1995, Vol. 3, pp. 1975–1980.
[31] WIERZCHOLSKI K., *Oil velocity and pressure distribution in short journal bearing under Rivlin Ericksen lubrication*, SAMS, System Analysis Modeling and Simulations, OPA Overseas Publishers Assoc., N.V., 1998, Vol. 32, pp. 205–228.
[32] WIERZCHOLSKI K., *The method of solutions for hydrodynamic lubrication by synovial fluid flow in human joint gap*, Control and Cybernetics, 2002, Vol. 31, No. 1, pp. 91–116.
[33] WIERZCHOLSKI K., *Capacity of deformed human hip joint gap in time dependent magnetic field*, Acta of Bioengineering and Biomechanics, 2003, Vol. 5, No. 1, pp. 43–65.
[34] WIERZCHOLSKI K., *Pressure distribution in human joint gap for elastic cartilage and time dependent magnetic field*, Russian Journal of Biomechanics, Perm, 2003, Vol. 7, No. 1, pp. 24–46.
[35] WIERZCHOLSKI K., *Tribologie für menschliche Gelenke*, Tribologie und Schmierungstechnik, 2002, 5, pp. 5–13.
[36] WIERZCHOLSKI K., *Theory of viscoelastic lubrication of hip joint in stochastic description for periodic motion*, Tribologia, 2004, 4(196), pp. 327–338.
[37] WOO S.-Y., JOHNSON G.A., SMITH B.A., *Mathematical Modeling of Ligaments and Tendons*, Journal Biomechanical Engineering, 1993, 115, pp. 468–473.

[38] XIAO H., BRUHNS O.T., MEYERS A., *Hypo-elasticity model based upon the logarithmic stress rate*, J. Elast., 1997, 47, pp. 51–68.